

University of Groningen

Transcriptome analysis reveals the contribution of oligodendrocyte and radial glia-derived cues for maintenance of microglia identity

Timmerman, Raissa; Zuiderwijk-Sick, Ella A.; Oosterhof, Nynke; 't Jong, Anke E.J.; Veth, Jennifer; Burm, Saskia M.; van Ham, Tjakko J.; Bajramovic, Jeffrey J.

Published in:
Glia

DOI:
[10.1002/glia.24136](https://doi.org/10.1002/glia.24136)

IMPORTANT NOTE: You are advised to consult the publisher's version (publisher's PDF) if you wish to cite from it. Please check the document version below.

Document Version
Publisher's PDF, also known as Version of record

Publication date:
2022

[Link to publication in University of Groningen/UMCG research database](#)

Citation for published version (APA):

Timmerman, R., Zuiderwijk-Sick, E. A., Oosterhof, N., 't Jong, A. E. J., Veth, J., Burm, S. M., van Ham, T. J., & Bajramovic, J. J. (2022). Transcriptome analysis reveals the contribution of oligodendrocyte and radial glia-derived cues for maintenance of microglia identity. *Glia*, 70(4), 728-747. <https://doi.org/10.1002/glia.24136>

Copyright

Other than for strictly personal use, it is not permitted to download or to forward/distribute the text or part of it without the consent of the author(s) and/or copyright holder(s), unless the work is under an open content license (like Creative Commons).

The publication may also be distributed here under the terms of Article 25fa of the Dutch Copyright Act, indicated by the "Taverne" license. More information can be found on the University of Groningen website: <https://www.rug.nl/library/open-access/self-archiving-pure/taverne-amendment>.




Take-down policy

If you believe that this document breaches copyright please contact us providing details, and we will remove access to the work immediately and investigate your claim.

Downloaded from the University of Groningen/UMCG research database (Pure): <http://www.rug.nl/research/portal>. For technical reasons the number of authors shown on this cover page is limited to 10 maximum.

RESEARCH ARTICLE

Transcriptome analysis reveals the contribution of oligodendrocyte and radial glia-derived cues for maintenance of microglia identity

Raissa Timmerman¹  | Ella A. Zuiderwijk-Sick¹ | Nynke Oosterhof^{2,3} |
Anke E. J. 't Jong¹ | Jennifer Veth¹ | Saskia M. Burm¹ | Tjakko J. van Ham²  |
Jeffrey J. Bajramovic¹ 

¹Alternatives Unit, Biomedical Primate Research Centre, Rijswijk, The Netherlands

²Department of Clinical Genetics, Erasmus MC, University Medical Center Rotterdam, Rotterdam, The Netherlands

³European Research Institute for the Biology of Ageing, University Medical Center Groningen, Groningen, The Netherlands

Correspondence

Jeffrey J. Bajramovic, Alternatives Unit, Biomedical Primate Research Centre, Lange Kleiweg 161, 2288 GJ Rijswijk, The Netherlands.
Email: bajramovic@bprc.nl

Abstract

Microglia are increasingly being recognized as druggable targets in neurodegenerative disorders, and good *in vitro* models are crucial to address cell biological questions. Major challenges are to recapitulate the complex microglial morphology and their *in vivo* transcriptome. We have therefore exposed primary microglia from adult rhesus macaques to a variety of different culture conditions including exposure to soluble factors as M-CSF, IL-34, and TGF- β as well as serum replacement approaches, and compared their morphologies and transcriptomes to those of mature, homeostatic *in vivo* microglia. This enabled us to develop a new, partially serum-free, monoculture protocol, that yields high numbers of ramified cells. We also demonstrate that exposure of adult microglia to M-CSF or IL-34 induces similar transcriptomes, and that exposure to TGF- β has much less pronounced effects than it does on rodent microglia. However, regardless of culture conditions, the transcriptomes of *in vitro* and *in vivo* microglia remained substantially different. Analysis of differentially expressed genes inspired us to perform 3D-spherical coculture experiments of microglia with oligodendrocytes and radial glia. In such spheres, microglia signature genes were strongly induced, even in the absence of neurons and astrocytes. These data reveal a novel role for oligodendrocyte and radial glia-derived cues in the maintenance of microglial identity, providing new anchor points to study microglia in health and disease.

KEYWORDS

IL-34, M-CSF, microglia, oligodendrocytes, serum, TGF- β , transcriptome

1 | INTRODUCTION

Microglia, the resident tissue macrophages of the central nervous system (CNS), are key players during brain development, homeostasis and disease (Aloisi, 2001; Bajramovic, 2011; Li & Barres, 2018; Paolicelli et al., 2011). Activation or dysfunction of microglia is linked to classical neuroinflammatory diseases such as viral encephalitis and

multiple sclerosis (MS), but also to neurodegenerative diseases like Alzheimer's disease (AD), Parkinson's disease, Huntington's disease and amyotrophic lateral sclerosis (Hall et al., 1998; Haukedal & Freude, 2019; Heneka et al., 2014; Kim & Joh, 2006; McGeer et al., 1988; Perry et al., 2010). In addition, many of the genes recently identified as risk factors for the development of AD in genome-wide association studies, such as *APOE*, *TREM2*, and *CD33*, are expressed

by microglia (Crotti & Ransohoff, 2016; Karch & Goate, 2015; Zhang et al., 2016). Microglia, therefore, represent promising cellular targets for therapeutic intervention in neuroinflammatory and neurodegenerative diseases.

To obtain detailed cellular biological knowledge of microglia, good *in vitro* models are instrumental. Different *in vitro* systems have been developed over time, ranging from cell lines to primary microglia to stem cell-derived microglia-like cells, all with their own characteristic features (Timmerman et al., 2018). Primary microglia cultures, although laborious and relatively short-lived, have among others been used to provide insight into tissue-specific features of innate immune responses (Burm et al., 2015, 2016; Timmerman et al., 2021). Recent studies have however demonstrated that there are important differences in the morphology and the transcriptome of primary *in vitro* microglia as compared to those of mature homeostatic *ex vivo* microglia, both in humans and in rodents (Bohlen et al., 2017; Butovsky et al., 2014; Gosselin et al., 2017; Mizze et al., 2017). The expression levels of a variety of gene products were found to differ and most importantly, expression of many of the microglia signature genes (Bennett et al., 2016; Butovsky et al., 2014; Galatro, Vainchtein, et al., 2017; Gosselin et al., 2017; Olah et al., 2018; Patir et al., 2019; Zhang et al., 2014; Zhang et al., 2016), such as *P2RY12*, *TMEM119*, and *GPR34* was lost *in vitro*.

Multiple studies have been devoted to the optimization of primary microglia cultures. Gene knockout studies have demonstrated the importance of colony stimulating factor-1 (CSF-1) receptor-induced signaling for microglial proliferation and survival (Erblich et al., 2011). There are two reported ligands for the CSF-1 receptor, macrophage colony-stimulating factor (M-CSF) and interleukin (IL)-34, and at present it is not known whether primary microglia exposed to either growth factor develop differently. In addition, transcriptome comparisons of *ex vivo* and primary rodent microglia have pinpointed the importance of exposure to transforming growth factor beta (TGF- β) to induce the expression of the adult microglial gene expression profile (Butovsky et al., 2014), but its importance for primary microglia of primate origin remains to be established. Finally, it was recently reported that exposure of primary microglia to serum profoundly alters their gene expression profile, and a new serum-free culture medium has been developed (Bohlen et al., 2017). Despite these advances, important challenges remain to culture microglia that resemble the complex ramified morphology of *in vivo* microglia and express the signature genes that determine microglial identity.

We here analyzed the cellular morphologies and the transcriptomes of primary microglia that were cultured under different conditions, and compared these to *ex vivo* microglia. To bridge the gap between rodents and humans, we isolated primary microglia from rhesus macaques, outbred animals that are evolutionary close to humans (Burm et al., 2015, 2016; Van Der Putten et al., 2012; Zuiderwijk-Sick et al., 2007). We exposed adult rhesus microglia to M-CSF and IL-34, both in the presence and absence of TGF- β . We also explored different serum exposure and washout culture regimes, and finally, we have experimented with a co-culture system containing microglia, oligodendrocytes, and radial glia. We report the

development of a new, partially serum-free, monoculture protocol that yields high numbers of ramified cells. In addition, our co-culture system revealed an unexpected role for oligodendrocyte and radial glia-derived cues in the maintenance of microglial identity.

2 | MATERIALS AND METHODS

2.1 | Animals

Brain tissue was obtained from adult rhesus macaques (*Macaca mulatta*) without neurological disease that became available from the outbred breeding colony. No animals were sacrificed for the exclusive purpose of microglia isolation. Better use of experimental animals contributes to the priority 3Rs program of the Biomedical Primate Research Centre. Individual identification data of the animals are listed in Table 1.

2.2 | Primary cell isolation

Ex vivo microglia isolation was carried out as described previously (Galatro, Vainchtein, et al., 2017). Frontal subcortical white matter samples were collected in *ex vivo* microglia medium (EMM) comprised of HBSS (Gibco Life Technologies, Bleiswijk, The Netherlands) supplemented with 15 mM HEPES (Lonza, Cologne, Germany) and 0.6% (wt/vol) glucose (Sigma-Aldrich, Saint Louis, MO). Meninges and blood vessels were removed manually. The brain tissue was dissociated in a glass tissue homogenizer and filtered using a 300 μ m sieve followed by a 106 μ m sieve to obtain a single-cell suspension. Cells were pelleted by centrifugation at 220g for 10 min at 4°C. The pellet was resuspended in 22% (vol/vol) Percoll (Cytiva, Uppsala, Sweden), 37 mM NaCl and 75% (vol/vol) myelin gradient buffer (5.6 mM NaH₂PO₄, 20 mM Na₂HPO₄, 140 mM NaCl, 5.4 mM KCl, 11 mM glucose, pH 7.4). A layer of PBS (Gibco) was added on top, and this gradient was centrifuged at 950g for 20 min at 4°C (minimal acceleration, no brake). The myelin layer and the remaining supernatant were carefully removed and the pellet was resuspended in a solution of 60% Percoll, which was overlaid with 30% Percoll and layered with PBS, respectively, and centrifuged at 800g for 25 min at 4°C (minimal acceleration, no brake). The cell layer at the 60%–30% Percoll interphase was collected with a Pasteur pipette, washed with EMM and centrifuged at 600g for 10 min at 4°C. The final pellet was resuspended in HBSS without phenol red (Gibco) supplemented with 15 mM HEPES, 0.6% glucose and 1 mM EDTA (Invitrogen; Life technologies). Fc receptors were blocked with human Fc receptor binding inhibitor (eBioscience, Thermo Fisher Scientific, Cat#14-9161-73, RRID:AB_468582, Waltham, MA) for 15 min on ice. For fluorescence-activated cell sorting, cells were incubated for 25 min on ice, in the dark, with anti-human CD11b-PE (1:25, Clone: ICRF44, BioLegend, Cat#301306, RRID:AB_314158, Uithoorn, The Netherlands) and anti-rhesus CD45-FITC (1:25, Clone: MB4-6D6, Miltenyi Biotec, Cat# 130-091-898, RRID:AB_244324 Bergisch Gladbach, Germany).

TABLE 1 Individual identification data of rhesus macaques

Donor nr.	Monkey ID nr.	Age (years)	Sex	Weight (kg)	Origin	Condition
1	R11065	5	Male	11,0	India	In vitro
2	R14033	2	Male	2,7	India	In vitro
3	R09080	7	Female	6,0	India	In vitro
4	R12102	4	Female	4,0	India	In vitro
5	R09105	7	Female	5,6	India	Ex vivo
6	R08072	8	Male	10,6	India	Ex vivo
7	R08094	8	Male	11,6	India	Ex vivo
8	R07015	9	Male	12,2	India	Ex vivo
9	R11110	7	Female	7,8	India	In vitro
10	R15031	3	Female	4,3	India	In vitro
11	R15028	3	Male	6,3	India	In vitro
12	R14052	4	Male	6,4	India	In vitro
13	R04030	15	Female	6,4	India	In vitro
14	R08124	11	Female	5,1	India	In vitro
15	R08130	11	Female	5,5	India	In vitro
16	R08007	12	Female	6,3	Mix	In vitro
17	R05080	14	Female	5	India	In vitro
18	R06005	13	Female	8,2	India	In vitro
19	R97062	22	Female	7,5	India	In vitro

Subsequently, cells were washed with HBSS without phenol red and centrifuged at 300g for 3 min at 4°C. The cells were passed through a 35 µm nylon mesh, collected in round-bottom tubes (Corning Costar Europe, Badhoevedorp, the Netherlands) and sorted using a Beckman Coulter MoFloAstrio cell sorter. Cells were sorted based on CD11b^{high}/CD45^{int} expression and negative staining for DAPI or the LIVE/DEAD Fixable Red Dead Cell stain (Thermo Fisher Scientific) and collected in RNeasy lysis buffer (Qiagen GmbH, Hilden, Germany). Sorted cells were centrifuged at 5000g for 10 min and pellets were lysed in RLT-Plus buffer (Qiagen) for RNA extraction.

Microglia for primary cell cultures were isolated as described previously with a few modifications (Burm et al., 2015; van der Putten et al., 2009; Zuiderwijk-Sick et al., 2007). In short, Frontal subcortical white matter samples were collected in primary microglia medium (PMM) comprised of 1:1 v/v DMEM (high glucose)/HAM F10 Nutrient mixture (Gibco) supplemented with 10% v/v heat-inactivated FBS (TICO Europe, Amstelveen, The Netherlands), 2 mM glutamax, 50 units/ml penicillin and 50 µg/ml streptomycin (all from Gibco). microglia isolations were initiated from cubes of ~4.5 g tissue that were depleted of meninges and blood vessels manually. Tissue was chopped into cubes of less than 2 mm² by using gentleMACS™ C tubes (Miltenyi Biotec) and incubated at 37°C for 20 min in PBS containing 0.25% (w/v) trypsin (Gibco) and 1 mg/ml bovine pancreatic DNase I (Sigma-Aldrich) and mixed every 5 min. The supernatant was discarded (no centrifugation), the pellet was washed in PMM and passed over a 100 µm nylon cell strainer (Falcon; Becton Dickinson Labware Europe) and centrifuged for 7 min at 524g. The pellet was resuspended in 22% (vol/vol) Percoll, 37 mM NaCl and 75% (vol/vol) myelin gradient buffer (5.6 mM NaH₂PO₄, 20 mM Na₂HPO₄, 137 mM

NaCl, 5.3 mM KCl, 11 mM glucose, 3 mM BSA fraction V, pH 7.4). A layer of myelin gradient buffer was added on top, and this gradient was centrifuged at 1561g for 25 min (minimal brake). The pellet was washed in PMM and centrifuged for 7 min at 524g. Cells were plated at a density of 6.5 × 10⁴ cells/cm² in tissue-culture treated well plates (Corning Costar Europe) in PMM. For sphere cultures, cells were plated at a density of 10.5 × 10⁴ cells/cm² in ultra-low attachment plates (Corning Costar Europe) and placed on a Hi/Lo shaker (IBI Scientific, Dubuque, IA) at 15 rpm.

2.3 | Cell culture

2.3.1 | Microglia monoculture

After overnight incubation at 37°C in a humidified atmosphere containing 5% CO₂, unattached cells and myelin debris were removed by washing with PBS and replaced by fresh standard medium (SM; Table S1) comprised of 1:1 v/v DMEM (high glucose)/HAM F10 Nutrient mixture supplemented with 10% v/v heat-inactivated FBS, 2 mM glutamax, 50 units/ml penicillin and 50 µg/ml streptomycin supplemented with 20 ng/ml (≥ 4 units/ml) M-CSF (PeproTech, London, UK) or 100 ng/ml IL-34 (Peprotech), with or without 12.5 ng/ml TGF-β1 (Miltenyi Biotec) or replaced by fresh serum-free microglial (SFM; Table S1) culture medium comprised of DMEM/F12 (Gibco) supplemented with 0.5 mM glutamax, 50 units/ml penicillin, 50 µg/ml streptomycin, 5 µg/ml N-acetyl-L-cysteine (Sigma-Aldrich), 5 µg/ml insulin (Sigma-Aldrich), 100 µg/ml apo-transferrin (Sigma-Aldrich), 100 ng/ml sodium selenite (Sigma-Aldrich), 20 ng/ml

(≥ 4 units/ml) M-CSF, 12.5 ng/ml TGF- $\beta 1$, 1.5 $\mu\text{g/ml}$ ovine wool cholesterol (Avanti Polar Lipids, Alabaster, AL), 1 $\mu\text{g/ml}$ heparan sulfate (Galen Laboratory Supplies, North Haven, CT), 0.1 $\mu\text{g/ml}$ oleic acid (Cayman Chemical, Ann Arbor, MI), 1 ng/ml gondoic acid (Cayman Chemical).

2.3.2 | SM culture

All cells were kept in culture for 8 days without passaging. Half of the medium was replaced by fresh SM containing new growth factors every 3 days.

2.3.3 | SFM culture

All cells were kept in culture for 8 or 22 days without passaging. Half of the medium was replaced by fresh SFM medium containing new growth factors every 2–3 days.

2.3.4 | SM culture followed by SFM culture

All cells were kept in culture for 8, 15, or 22 days without passaging. Cells were exposed to SM for the first 4 days. At day 4, cells were washed twice with PBS and replaced by SFM medium. From day 4, half of the medium was replaced by fresh SFM medium containing new growth factors every 2–3 days.

2.3.5 | Microglia sphere culture

Cells were incubated overnight at 37°C in a humidified atmosphere containing 5% CO₂, whereafter 20 ng/ml M-CSF was added. At day 4, spheres were carefully transferred to a new well containing SFM and were kept in culture for 11 additional days without passaging. Half of the culture medium was carefully replaced by fresh SFM containing new growth factors every 2–3 days.

2.4 | RNA extraction and library synthesis

Total cellular RNA was isolated using the RNeasy minikit (Qiagen) according to manufacturer's protocol. For donor nr. 1–12 (Table 1) the NEBNext Ultra Directional RNA Library Prep Kit for Illumina (New England Biolabs, Ipswich, MA) was used to prepare and process the samples. Briefly, mRNA was isolated from total RNA using oligo(dT) magnetic beads. After fragmentation of the mRNA, cDNA synthesis was performed followed by ligation of sequencing adapters and PCR amplification. The quality and yield after sample preparation were measured with a fragment analyzer (Agilent Technologies, Amstelveen, The Netherlands). Clustering and sequencing using the Illumina NextSeq 500 was performed according to manufacturer's protocols.

For donor nr. 13–16 (Table 1) The NEBNext Low Input RNA Library Prep Kit for Illumina (New England Biolabs) was used to process the samples. The sample preparation was performed according to manufacturer's protocol. Briefly, cDNA was synthesized and amplified from poly A tailed mRNA followed by ligation with the sequencing adapters and PCR amplification. The quality and yield after sample preparation was measured with the Fragment Analyzer (Agilent Technologies). Clustering and sequencing using the Illumina NovaSeq 6000 was performed according to manufacturer's protocols.

Prior to alignment, the reads were trimmed for adapter sequences using Trimmomatic v0.30. Presumed adapter sequences were removed from the read when the bases matched a sequence in the adapter sequence set (TruSeq adapters) with 2 or less mismatches and an alignment score of at least 12.

The *Macaca mulatta* genomic reference (Macaca_mulatta.Mmul_8.01.dna.toplevel.fa) was used for alignment of the reads for each sample. The reads were mapped to the reference sequence using a short read aligner based on Burrows-Wheeler Transform (Tophat v2.0.14) with default settings. SAMtools v1.3 package (<http://htslib.org/>, RRID:SCR_002105) was used to sort and index the BAM files. Based on the mapped locations in the alignment file the frequency of how often a read was mapped on a transcript was determined with HTSeq v0.6.1p1 (http://htseq.readthedocs.io/en/release_0.9.1/, RRID:SCR_005514). The counts were saved to count files, which served as input for downstream RNA sequencing analysis.

2.5 | Bioinformatics

Bioconductor Package (<https://bioconductor.org/packages/release/bioc/html/biomaRt.html>, RRID:SCR_019214) was used to annotate the genes and to generate a gene symbol list (Durinck et al., 2005, 2009). The accession number for the gene level RNA-sequencing data from freshly isolated microglia and cultured primary microglia from rhesus macaques reported in this paper is GEO: GSE171476.

Data were inspected using principal component analysis (PCA) and heatmaps generated with heatmap.2 of Bioconductor package gplots. Differential gene expression analysis was performed with Bioconductor package EdgeR (<https://bioconductor.org/packages/release/bioc/html/edgeR.html>, RRID:SCR_012802) (Robinson et al., 2010). An overview of all performed differential gene expression analyses can be found in Table S2. Qiagen's Ingenuity Pathway Analysis (Qiagen, <https://www.qiagenbioinformatics.com/products/ingenuity-pathway-analysis>, RRID:SCR_008653) was used to perform pathway analysis. The Molecular Signatures Database (MsigDB, <http://software.broadinstitute.org/gsea/msigdb/index.jsp>, RRID:SCR_016863) was used to perform gene ontology analysis and canonical pathway analysis (Liberzon et al., 2011; Subramanian et al., 2005).

To infer the relative abundance of different CNS cell types in spheres, we used CIBERSORT (<https://cibersort.stanford.edu/>, RRID:SCR_016955) (Newman et al., 2015), a bioinformatic algorithm that allows calculation of cell types composition from gene expression

profiles. For the signature gene expression file, expression levels of neurons, astrocytes, microglia and oligodendrocytes of GEO: GSE73721 was used (Zhang et al., 2016). For the expression of radial glia signature genes, the transcriptome dataset of Pollen and colleagues was used (Pollen et al., 2015). All CIBERSORT analyses had *p* values of less than .05. The proportion of the CNS cell types in spheres are displayed in bar plots.

2.6 | Immunofluorescence and morphological analysis of monocultured microglia

Cells grown on glass coverslips were fixed for 30 min at RT in 2% PFA in PBS (Affymetrix, Santa Clara, CA), rinsed with PBS and PBS + 0.02% Tween20 (Sigma), respectively, and aspecific binding was blocked by incubation for 30 min in PBS containing 2% normal donkey serum (Abcam, Cambridge, UK). Samples were incubated overnight at 4°C with CX3CR1 antibody (1:400, Abcam, Cat#ab8021, RRID: AB_306203) in PBS containing 0.1% BSA (Sigma), rinsed with PBS + 0.02% Tween20, and incubated for 1 h at RT with donkey anti rabbit-FITC (1:400, Jackson ImmunoResearch Laboratories, Weste Grove, PA, Cat#711-095-152, RRID:AB_2315776) in PBS containing 0.1% BSA. After extensive washes with PBS, coverslips were mounted using ProLong™ Diamond Antifade + DAPI (Thermo Fisher Scientific) and images were acquired using a Leica DMI6000 fluorescence microscope and LASX software.

Microglial complexity was analyzed using Sholl and fractal analysis. In brief, CX3CR1-positive cell branches were traced using the Simple Neurite Tracer plugin (Longair et al., 2011) in ImageJ (<https://imagej.nih.gov/ij/>, RRID:SCR_002285) and skeletonized. Of these skeletonized traces, branch intersections with concentric circles per 5 μm steps from the nucleus were counted using a Sholl analysis plugin (Ferreira et al., 2014). Numbers of intersections were averaged per donor and plotted. Subsequently, the area under the curve (AUC) was extracted in which higher AUC values reflect a higher complexity. For fractal analysis, the FracLac plugin (<https://imagej.nih.gov/ij/plugins/fracLac/FLHelp/Introduction.htm>) for ImageJ was used. Skeletonized images were converted to outlines and fractal dimensions (D_B) of each cell were analyzed as described earlier (Morrison et al., 2017; Young & Morrison, 2018). FracLac calculated the D_B using a box counting protocol, summarized in the reference guide provided for FracLac for ImageJ: <https://imagej.nih.gov/ij/plugins/fracLac/FLHelp/BoxCounting.htm>. In brief summary, a cell is more complex as D_B approaches 2.

2.7 | Immunofluorescence of brain tissue and spheres

For formalin-fixed, paraffin-embedded brain tissue of adult rhesus macaques, 5 μm sections were collected on Superfrost Plus glass slides (VWR international, Leuven, Belgium), dried at 37°C, deparaffinized in xylene and rehydrated through a graded series of

ethanol concentrations. Endogenous peroxidase activity was quenched by incubating the slides for 20 min in 0.3% hydrogen peroxide, followed by rinsing in PBS and antigen retrieval by steaming in antigen retrieval buffer at pH 7.5 (IHC world, Woodstock, MD). Slides were cooled to room temperature and rinsed in PBS again. To block aspecific binding, slides were incubated with 10% normal donkey serum (Abcam) in PBS for 20 min at room temperature.

For Tissue-Tek embedded spheres, 2% PFA-fixed 8 μm sections were collected on Superfrost Plus glass slides (VWR), fixed in acetone for 10 min at room temperature, and washed in PBS. Aspecific binding was blocked by incubation with 2% normal donkey serum (Abcam) in PBS for 20 min at room temperature.

Brain tissue and sphere sections were incubated overnight at 4°C with primary antibodies in PBS containing 0.1% BSA (Sigma). Primary antibodies used were anti-Tenascin C (1:50, R and D Systems, Minneapolis, MN, Cat#MAB2138, RRID:AB_2203818), anti-GFAP (1:50, Sigma-Aldrich, Cat#SAB5201104, RRID:AB_2827276), anti-IBA1 (1:50, Wako Pure Chemical Industries, Osaka, Japan, Cat#019-19741, RRID:AB_839504) and anti-MBP (1:100, Novus Biologicals, Centennial, CO, Cat#MAB4269, RRID:AB_10552058). Next, sections were rinsed with PBS and incubated with either Alexa-488 or -594-labeled secondary antibodies (1:400; Jackson ImmunoResearch Laboratories, Cat#712-546-153, RRID:AB_2340686; Cat#711-545-152, RRID:AB_2313584; Cat#715-585-150, RRID:AB_2340854) for 90 min at room temperature. After extensive washes with PBS, slides were mounted using Prolonged Gold Antifade Mountant with DAPI (Thermo Fisher Scientific). Images were acquired using a Leica DMI6000 fluorescence microscope and LASX software.

2.8 | Statistics

GraphPad Prism 8.0 (<http://www.graphpad.com/>, RRID:SCR_002798) (GraphPad Software, San Diego, CA) was used for statistical analysis. Sholl analysis curves from which area under the curve data were deduced were created and analyzed using Graphpad Prism 8.0. Statistical details of experiments can be found in the figure legends.

3 | RESULTS

3.1 | Exposure of primary primate microglia to IL-34 and TGF-β has only moderate effects on their signature gene expression profile

Recent findings have demonstrated that exposure of primary rodent microglia to IL-34 and TGF-β supports cell cultures that better resemble in vivo microglia than exposure to M-CSF only does, which is the standard protocol. To assess whether this also applies to primary microglia from adult outbred primates, we analyzed cell morphologies and profiled the transcriptomes of primary microglia from four adult rhesus macaques that were exposed for 8 days to either M-CSF or IL-34, with or without TGF-β.

Microglial morphologies were highly similar for all different culture conditions (data not shown). Transcriptome analysis suggested that sex, and not culture condition, was the most important component to explain variance (15%) in the dataset (Figure 1a). Unsupervised hierarchical clustering using Spearman's correlation, further showed that samples from individual donors clustered together rather than samples from similar sex or similar culture conditions (Figure 1b). This demonstrates that the origin of the donor had more impact on the gene expression profiles of individual samples than the culture conditions did. Although variance is normal when working with outbred animals, we had anticipated that in vitro exposure for 8 days to a similar culture regime would have had more profound skewing effects.

We next performed in-depth analyses of the effects of the different culture variables on microglial gene expression. When comparing

M-CSF and IL-34-exposed microglia, not a single significant differentially expressed gene (DEG; FC ≥ 2 , FDR < 0.05) was found (Table 2). This implicates that M-CSF and IL-34 induce or sustain an almost identical gene expression profile in adult macaque primary microglia,

TABLE 2 Numbers of differentially expressed genes (DEG; FC ≥ 2 , FDR < 0.05) between primary microglia exposed for 8 days to either M-CSF or IL-34, with or without TGF- β

Comparisons	Total DEG
M-CSF vs. IL-34	0
M-CSF vs. M-CSF + TGF- β	297
IL-34 vs. IL-34 + TGF- β	168
IL-34 + TGF- β vs. M-CSF + TGF- β	0

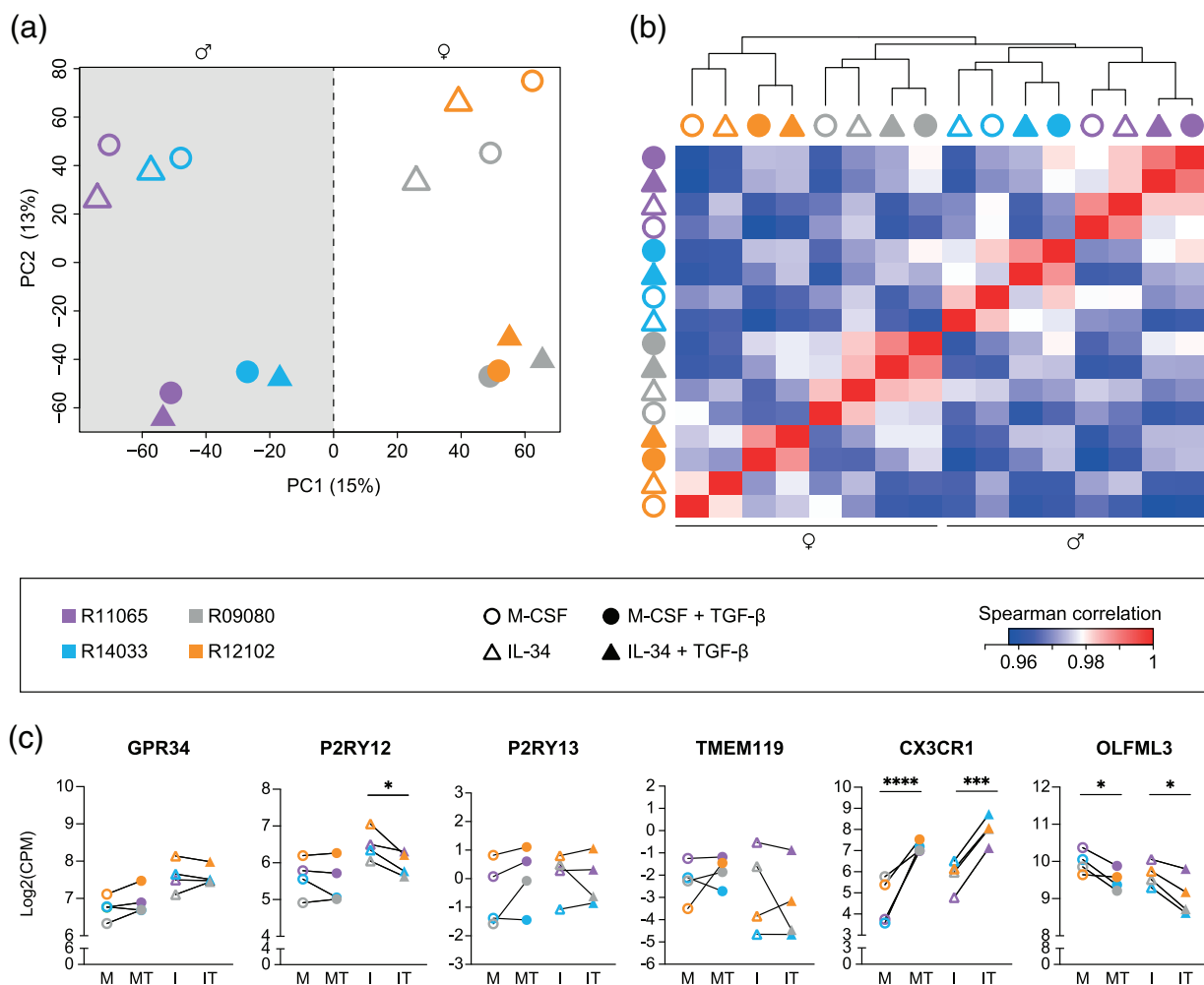


FIGURE 1 Effects of donor-donor variation and of M-CSF, IL-34, and TGF- β exposure on the transcriptomes of primary microglia. (a) Principal component analysis of the transcriptomes of primary microglia from four adult donors cultured under four different conditions (M-CSF, M-CSF + TGF- β , IL-34, and IL-34 + TGF- β). The first principal component is responsible for 15% of the variance in the dataset, whereas the second principal component is responsible for 13% of the variance. The symbols in the gray area are derived from male donors, whereas the symbols in the white area are derived from female donors. (b) Spearman's correlation heatmap of the transcriptome of cultured primary microglia. (c) Log-transformed expression (CPM) values of microglial signature genes. M = M-CSF, MT = M-CSF + TGF- β , I = IL-34, IT = IL-34 + TGF- β . EdgeR false discovery rates (FDR) are used to display statistical differences. $N = 4$ for each culture condition. *FDR < 0.05 , ***FDR < 0.005 , ****FDR < 0.001

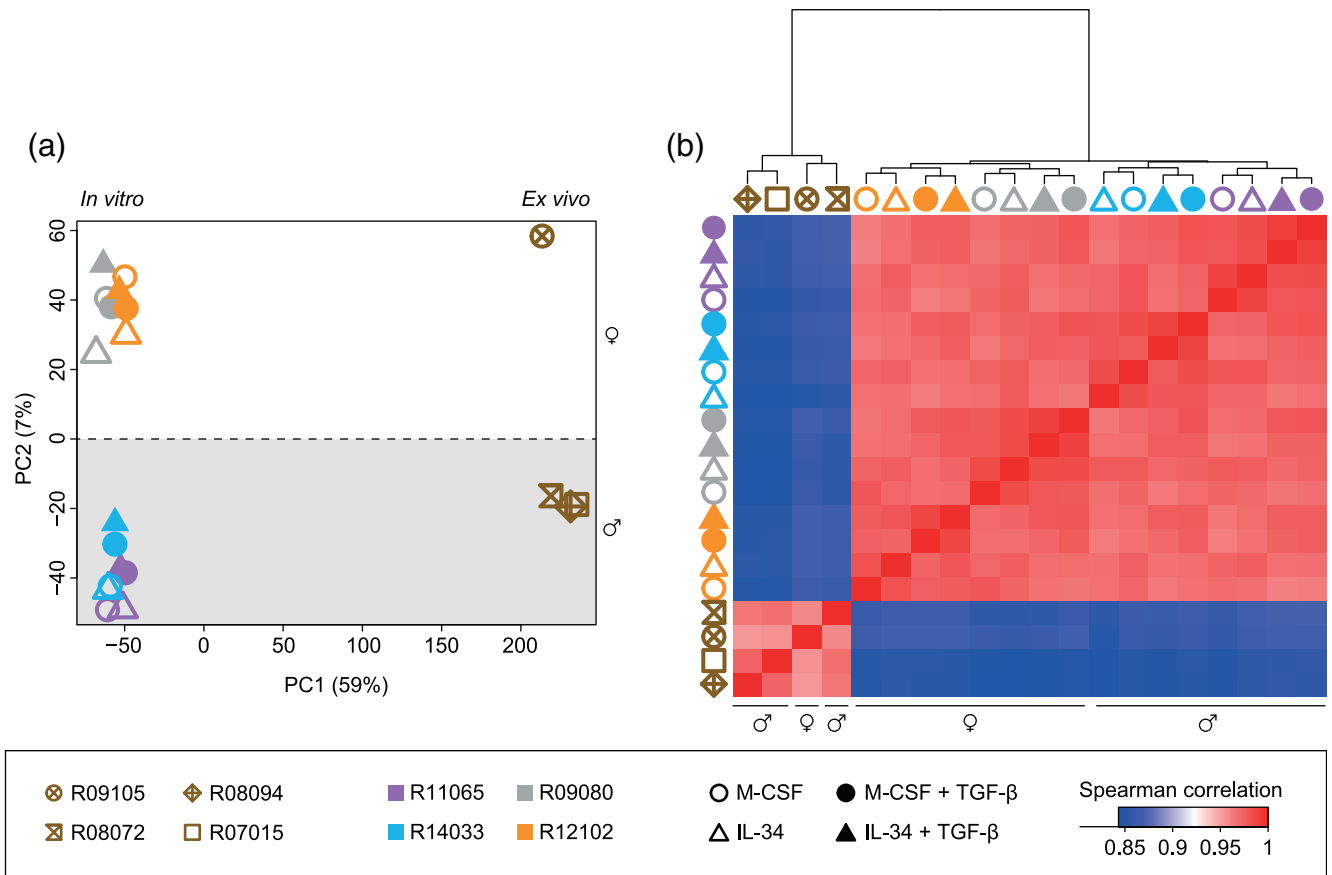


FIGURE 2 Transcriptome analysis of primary adult microglia and ex vivo microglia. (a) Principal component analysis of the transcriptome of ex vivo and in vitro microglia cultured under four different culture conditions. Ex vivo and in vitro microglia were derived from different donors. The first principal component is responsible for 59% of the variance in the dataset, whereas the second principal component is responsible for 7% of the variance. The symbols in the gray area are derived from male donors, whereas the symbols in the white area are derived from female donors. (b) Spearman's correlation heatmap of the transcriptomes of in vitro and ex vivo microglia. (c) Gene ontology analysis of differentially expressed genes upregulated in in vitro microglia as compared to ex vivo microglia. Biological processes associated with upregulated DEG were analyzed using the molecular signatures database (Liberzon et al., 2011; Subramanian et al., 2005) FDR = false discovery rate. (d) Expression values in counts per million (CPM) of well-known cell cycle genes in in vitro and ex vivo microglia. EdgeR false discovery rates (FDR) are used to display statistical differences. In vitro $n = 16$, ex vivo $n = 4$. Center lines indicate the mean, error bars represent SD, ****FDR < 0.001

Condition	# Genes up in vitro	# Genes down in vitro	Total DEG
M-CSF	1487	1771	3258
M-CSF + TGF- β	1410	1434	2844
IL-34	1499	1579	3077
IL-34 + TGF- β	1422	1685	3107

TABLE 3 Numbers of differentially expressed genes (DEG; FC \geq 4, FDR < 0.01) between different in vitro microglia cultures and ex vivo microglia

which is consistent with data from adult human primary microglia (Walker et al., 2017). When we focused on the effects of TGF- β , we found that exposure to TGF- β was the second important component to explain variance (13%) in our data set (Figure 1a). DEG analyses reveal that the expression levels of 297 genes differed significantly between M-CSF and M-CSF + TGF- β -exposed microglia, and that the expression levels of 168 genes differed significantly between IL-34 and IL-34 + TGF- β -exposed microglia (Table 2, Figure S1 and Table S2). Since TGF- β has been described as pivotal for the expression of microglia signature genes in rodents (Butovsky et al., 2014; Gosselin et al., 2017), we analyzed the log-transformed RNA expression data of six described human and rodent microglia signature genes *GPR34*, *P2RY12*, *P2RY13*, *TMEM119*, *CX3CR1*, and *OLFML3*. Surprisingly, only *CX3CR1* was significantly upregulated after TGF- β exposure, both in combination with M-CSF and IL-34 (Figure 1c). *OLFML3*, a gene described to be positively regulated by TGF- β in mice (Butovsky et al., 2014; Neidert et al., 2018), was even significantly downregulated after TGF- β exposure, and also *P2RY12* was downregulated when microglia were exposed to TGF- β in combination with IL-34. We used two pathway analysis applications (IPA and MsigDB) to verify that the TGF- β pathway had indeed been activated (Table S3).

3.2 | Regardless of culture conditions, in vitro microglia are characterized by a proliferative phenotype as compared to in vivo microglia

We next compared the transcriptomes of our in vitro samples with those of ex vivo microglia that were freshly isolated using FACS sorting. In line with published data, major differences in the gene expression profiles of in vitro and ex vivo microglia were observed, regardless of cell culture conditions (Figure 2a and Table 3). The most important component explaining 59% of the variance between the samples, was the in vitro-ex vivo parameter. The second important component explaining 7% of the variance, was as expected sex (Figure 2a). Hierarchical clustering of the in vitro and ex vivo samples demonstrates the profoundness of the in vitro-ex vivo difference (Figure 2b), whereas DEG analyses of ex vivo microglia and the different in vitro microglia cultures (Figure S2 and Table S2) demonstrate that none of the culture regimes resulted in a transcriptome that better reflected the ex vivo transcriptome (Table 3), or resulted in a better mimic of their signature gene expression profile (Figure S3).

In order to gain more insight in the biological processes that were affected in vitro, we performed a gene set enrichment analysis for

genes that were upregulated in vitro (Liberzon et al., 2011; Subramanian et al., 2005). Genes upregulated in vitro were linked to gene ontology terms associated with the cell cycle, such as “mitotic cell cycle”, “cell cycle”, and “cell cycle process”. In addition, evidence was found for biological processes associated with cell movement, adhesion and structure (Figure 2c). RNA expression data confirmed that six well-described genes associated with the cell cycle were indeed upregulated in in vitro microglia compared to ex vivo microglia (Figure 2d). These results are in line with recent data of primary adult rat microglia, that were reported to upregulate among others the cell cycle pathway when they were exposed to serum (Bohlen et al., 2017).

3.3 | Short-term serum exposure, followed by a serum-free washout period supports the outgrowth of high numbers of microglia with a complex, ramified morphology

Bohlen and colleagues recently described a novel serum-free culture medium (SFM) containing M-CSF, TGF- β and cholesterol as the minimal supplements to allow survival of microglia in the absence of serum (Bohlen et al., 2017). We tested this SFM for culture of primary adult rhesus macaque microglia. Of note, microglia cultured with SFM were still exposed to serum during the isolation procedure and during the first 16 h after plating of the cells to facilitate cell adhesion. Complete elimination of serum during isolation and plating did not yield viable microglia cultures. Despite the presence of TGF- β and cholesterol, total cell yields after 8 days of culture were around 4-fold lower than with our 10% FCS-containing, standard microglia (SM) medium (Figure 3a). This decrease in cell number hampers downstream experimental analysis, and longer cell culture times did not improve cell yields (data not shown).

Consequently, we tested whether a short period of serum exposure, to facilitate initial survival and proliferation, followed by a period of serum-free washout could positively affect cell yields. We exposed microglia for 4 days to SM followed by exposure to SFM for 4, 11, or 18 days (Figure S4) and compared cell numbers to those of microglia exposed to SM for 8 days. We found that 4 days of serum exposure was sufficient to induce the outgrowth of cell numbers comparable to those obtained with SM, regardless of the duration of the serum-free washout period (Figure 3b). We also studied how different serum-free washout periods affected cellular morphology, using Sholl analysis. Serum-free washout periods of 11 and 18 days resulted in more complex cellular morphologies as compared to microglia cultured with SM

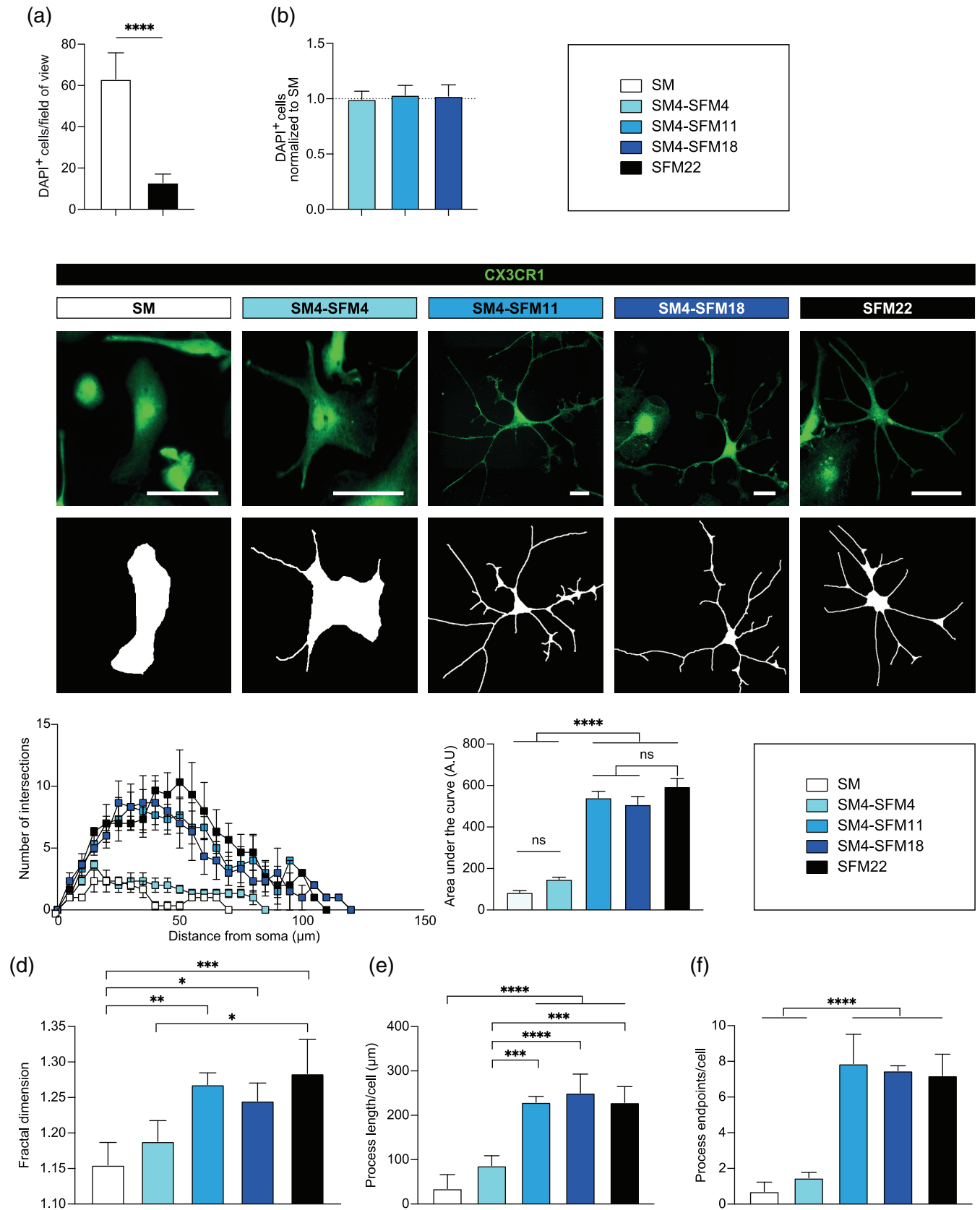


FIGURE 3 Legend on next page.

and SM4-SFM4 (Figure 3c) or microglia cultured on SM for 22 days (data not shown). In addition, serum-free washout periods for 11 and 18 days supported outgrowth of microglia with a comparably complex morphology as microglia exposed to SFM for 22 days (SFM22). The increased morphological complexity of microglia exposed to serum-free washout periods of 11 and 18 days, as compared to microglia exposed to SM, was confirmed by fractal dimension analysis (Figure 3d) where a higher fractal dimension is associated with a more complex cellular morphology (Morrison et al., 2017). We also quantified the number of microglia process length and endpoints per cell. Serum-free washout periods of 11 and 18 days resulted in a higher total process length per cell (Figure 3e) and in higher numbers of process endpoints (Figure 3f) as compared to microglia exposed to SM conditions or to a serum-free washout period of 4 days. In fact, total process length per cell and the number of process endpoints were comparable to microglia that were exposed to SFM for 22 days.

3.4 | Despite strongly reduced expression of cell cycling-associated gene products, the transcriptomes of serum-free microglia do not better mimic those of ex vivo microglia

Analysis of the transcriptomes by Spearman's correlation heatmap and DEG analyses demonstrated that the transcriptomes of SM4-SFM11 and SM4-SFM18 cultured microglia did not differ significantly from the transcriptomes of SFM22 microglia (Figure 4a, Table 4 and Figure S5). Furthermore, the expression levels of cell cycle genes were similar to those of SFM22 microglia (Figure 4b, in high resolution Figure S6). In addition, the cell cycle gene expression profiles of SM4-SFM11 and SM4-SFM18 microglia better mimicked those of ex vivo microglia than those of SM or SM4-SFM4 microglia.

We next compared the whole transcriptomes of SM, SM4-SFM4, SM4-SFM11, SM4-SFM18, and SFM22 cultured microglia (Figure S4) to the reference transcriptomes of ex vivo microglia that we used previously. The most important component to explain variance (58%) in our dataset was the ex vivo–in vitro parameter, whereas exposure to serum was the second principal component explaining 9% of the

variance (Figure 4c). Overall, the number of DEG ($FC \geq 4$, $FDR < 0.01$) between ex vivo samples and the different culture conditions was comparable (Table 5), regardless of whether cells had been exposed to serum or not. Heatmaps of the DEG between ex vivo microglia and the different culture conditions show that SM and SM4-SFM4 conditions cluster together, while SM4-SFM11, SM4-SFM18, and SFM22 rather cluster by donor (Figure S7). Eighty percent of the DEG between the SM condition and ex vivo microglia overlapped with the DEG between the SFM4-SFM11 condition and ex vivo microglia (data not shown). The expression of microglia signature genes was comparably different between all different culture conditions and ex vivo microglia (Figure S8). Although the use of SFM thus improved microglial cell morphology and the expression of cell cycling-associated gene products, their RNA expression profiles did not better mimic those of ex vivo microglia.

3.5 | A multicellular environment is important for maintenance of the in vivo microglia transcriptome

As the SM4-SFM11 protocol yielded high cell numbers with a ramified morphology and with a transcriptome indicative of reduced proliferative activity, we continued with this protocol as our reference. We performed new gene set enrichment analyses to gain further insights in the biological processes involved in the differences between in vitro and ex vivo microglia. We first analyzed the genes that were upregulated in vitro (Figure 4d) and observed that biological processes linked to cell movement, adhesion, morphology, and structure organization were most affected. For example, annexins, integrins, and matrix metalloproteinases (MMPs) related genes were all upregulated (Figure 4e). The upregulation of genes linked to these biological processes was not specific for microglia cultured under serum-free conditions, as it was also observed for microglia that had been exposed to serum (Figure 2c). Genes that were downregulated in vitro as compared to ex vivo were among others associated with the positive regulation of multicellular organismal processes, cell–cell signaling, regulation of cell differentiation and neurogenesis (Figure 4f). The lack of signals from other CNS cells might have contributed to this effect

FIGURE 3 Effects of short-serum exposure and serum-free washout regimes on microglia morphology. (a) Numbers of DAPI⁺ primary microglia cultured in SM or SFM medium for 8 days. Cell counting was performed in 20 random fields of view from three donors for each condition. Statistical differences were examined by paired Student's *t*-test. Error bars represent SD, *****p* < 0.001. (b) Numbers of DAPI⁺ primary microglia after 4 days SM exposure followed by a serum-free washout of 4 (SM4-SFM4), 11 (SM4-SFM11), and 18 (SM4-SFM18) days. DAPI⁺ cell numbers were normalized to DAPI⁺ cell numbers of microglia cultured with serum for 8 days (SM). Dashed line represents the average DAPI⁺ cells of SM cultured microglia. Statistical differences were examined by paired Student's *t*-test, *n* = 5 per culture condition. Error bars represent SD. (c) Representative pictures of microglia cultured under five different culture conditions (specified in Figure S4) and immunostained for the microglial marker CX3CR1. Scale bars are 50 μm. CX3CR1⁺ cells were skeletonized and the number of intersections per 5 μm steps from the nucleus were analyzed using Sholl analysis. Number of intersections were analyzed for 10 random cells and averaged per donor and plotted. Error bars represent SD, *n* = 3 for each condition. Sholl analysis-derived area under the curve was quantified (arbitrary units: (a).U.) in which higher area under the curve (AUC) values reflect a higher morphological complexity. Statistical AUC differences were examined by one-way ANOVA with Tukey's multiple comparisons test. Error bars represent standard error of the mean. *****p* < .001. (d) Fractal dimension, (e) process length/cell, and (f) process endpoints/cell of microglia cultured under different conditions. Analyses were performed on 10 random cells for each condition and averaged per donor. Statistical differences were examined by one-way ANOVA with Tukey's multiple comparisons test. *N* = 3, error bars represent SD, **p* < .05, ***p* < .01, ****p* < .005, *****p* < .001

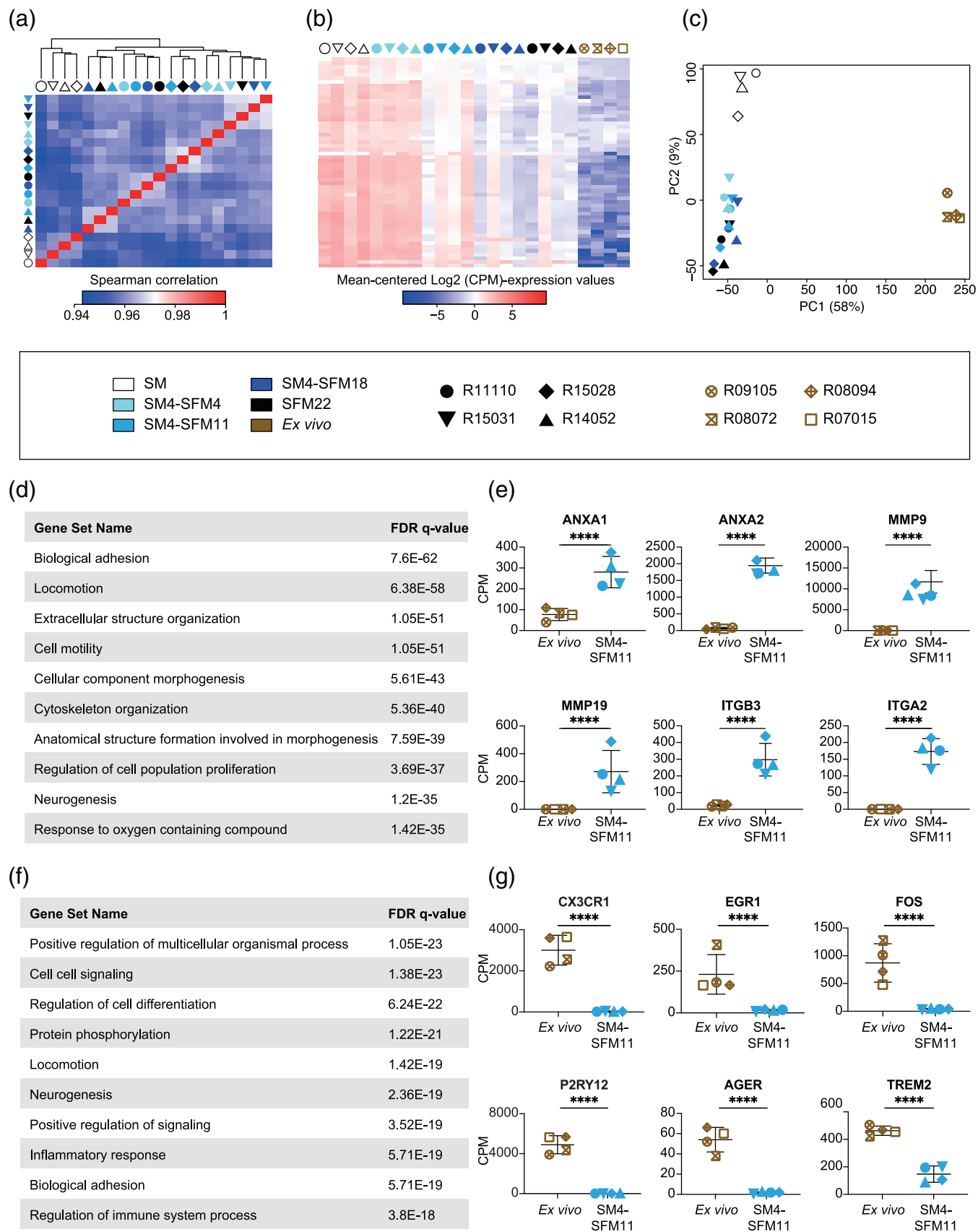


FIGURE 4 Legend on next page.

as microglial genes involved in crosstalk with other brain cells, such as *CX3CR1* (Sheridan & Murphy, 2013), *EGR1* (Veremeyko et al., 2019), *FOS* (Eun et al., 2004), *P2RY12* (Cserep et al., 2020), *AGER* (Matejuk & Ransohoff, 2020), and *TREM2* (Kober & Brett, 2017) are prominently present on this list of downregulated genes in vitro (Figure 4g). These findings were again not related to exposure to serum, as genes associated with these biological processes were also downregulated in microglia that had been exposed to serum (Table S4).

3.6 | Oligodendrocyte- and radial glia-derived cues induce the expression of microglia signature genes

Our initial cell suspension contains microglia as well as varying numbers of oligodendrocytes and CNS precursor cells, and we selectively favor the outgrowth of a > 98% pure primary microglia population by washing away non-adherent cells at day 1 (Zuiderwijk-Sick et al., 2007). We hypothesized that by plating our initial cell suspension in ultra-low attachment plates under continuous shaking, we might allow for survival and outgrowth of other cells. Indeed, this

resulted in the formation of spheres (Figure S9). To determine their cellular composition, we isolated RNA and analyzed the expression levels of CNS cell type-specific genes. These were then compared to their expression levels in SM4-SFM11 microglia derived from the same four adult rhesus macaques. We observed that microglial genes such as *TYROBP*, *GPR84*, and *PTPRC* were highly and comparably expressed in both conditions. On the other hand, oligodendrocytic, astrocytic and radial glial genes were expressed in spheres but virtually absent in monocultures of microglia (Figure 5a), demonstrating that sphere formation indeed allowed for the survival of multiple brain cell types. To estimate the abundance of CNS cell types in the spheres, we used CIBERSORT, a computational tool to quantify relative levels of distinct cell types within a complex gene expression admixture (Newman et al., 2015). The RNA expression profiles of microglia, neurons, oligodendrocytes, astrocytes, and radial glia were used to create a signature gene expression matrix (Pollen et al., 2015; Zhang et al., 2016). Use of this matrix in a CIBERSORT analysis leads to the estimation that the spheres consist for $\pm 50\%$ of microglia, $\pm 30\%$ of oligodendrocytes, and $\pm 10\%$ of radial glia (Figure 5b), and that astrocytes and neurons are not present. To validate the

	SM	SM4-SFM4	SM4-SFM11	SM4-SFM18	SFM22
SM	-	1500	1715	2028	2334
SM4-SFM4	1500	-	354	903	871
SM4-SFM11	1715	354	-	3	26
SM4-SFM18	2028	903	3	-	0
SFM22	2334	871	26	0	-

TABLE 4 Numbers of differentially expressed genes (DEG; FC ≥ 2 , FDR < 0.05) between the in vitro conditions SM, SM4-SFM4, SM4-SFM11, SM4-SFM18, and SFM22

Condition	# Genes up in vitro	# Genes down in vitro	Total DEG
SM	1589	1610	3199
SM4-SFM4	1710	1522	3232
SM4-SFM11	1619	1438	3057
SM4-SFM18	1601	1477	3078
SFM22	1721	1492	3213

TABLE 5 Numbers of differentially expressed genes (DEG; FC ≥ 4 , FDR < 0.01) between different in vitro microglia cultures and ex vivo microglia

Note: See Figure S4 for an overview of the culture conditions.

FIGURE 4 Transcriptome analysis of serum-free cultured microglia and ex vivo microglia. (a) Spearman's correlation heatmap of the transcriptomes of SM, SM4-SFM4, SM4-SFM11, SM4-SFM18, and SFM22 cultured microglia. (b) Heatmap of mean-centered Log₂(CPM)-expression values of cell cycle genes of SM, SM4-SFM4, SM4-SFM11, SM4-SFM18, and SFM22 cultured microglia and ex vivo microglia. (c) Principal component analysis of the transcriptomes of SM, SM4-SFM4, SM4-SFM11, SM4-SFM18, and SFM22 cultured microglia and ex vivo microglia. Ex vivo and in vitro microglia were derived from different donors. The first principal component explains 58% of the variance in the dataset, whereas the second principal component explains 9% of the variance. (d) Biological processes associated with differentially expressed genes (DEG) upregulated in SM4-SFM11 microglia compared to ex vivo microglia. Processes were analyzed using the molecular signatures database (MsigDB) (Liberzon et al., 2011; Subramanian et al., 2005). FDR = false discovery rate. (e) Expression values (CPM) of extracellular matrix-related genes (annexins, matrix metalloproteinases, and integrins) of ex vivo and SM4-SFM11 microglia. EdgeR false discovery rates (FDR) are used to display statistical differences, $n = 4$, center line indicates the mean, error bars represent SD, ****FDR < 0.001. (f) Biological processes associated with DEG downregulated in SM4-SFM11 microglia compared to ex vivo microglia. Processes were analyzed using the molecular signatures database. FDR = false discovery rate. (g) Expression values (CPM) of genes associated with microglia crosstalk of ex vivo and SM4-SFM11 microglia. EdgeR false discovery rates (FDR) are used to display statistical differences, $n = 4$, center line indicates the mean, error bars represent SD, ****FDR < 0.001

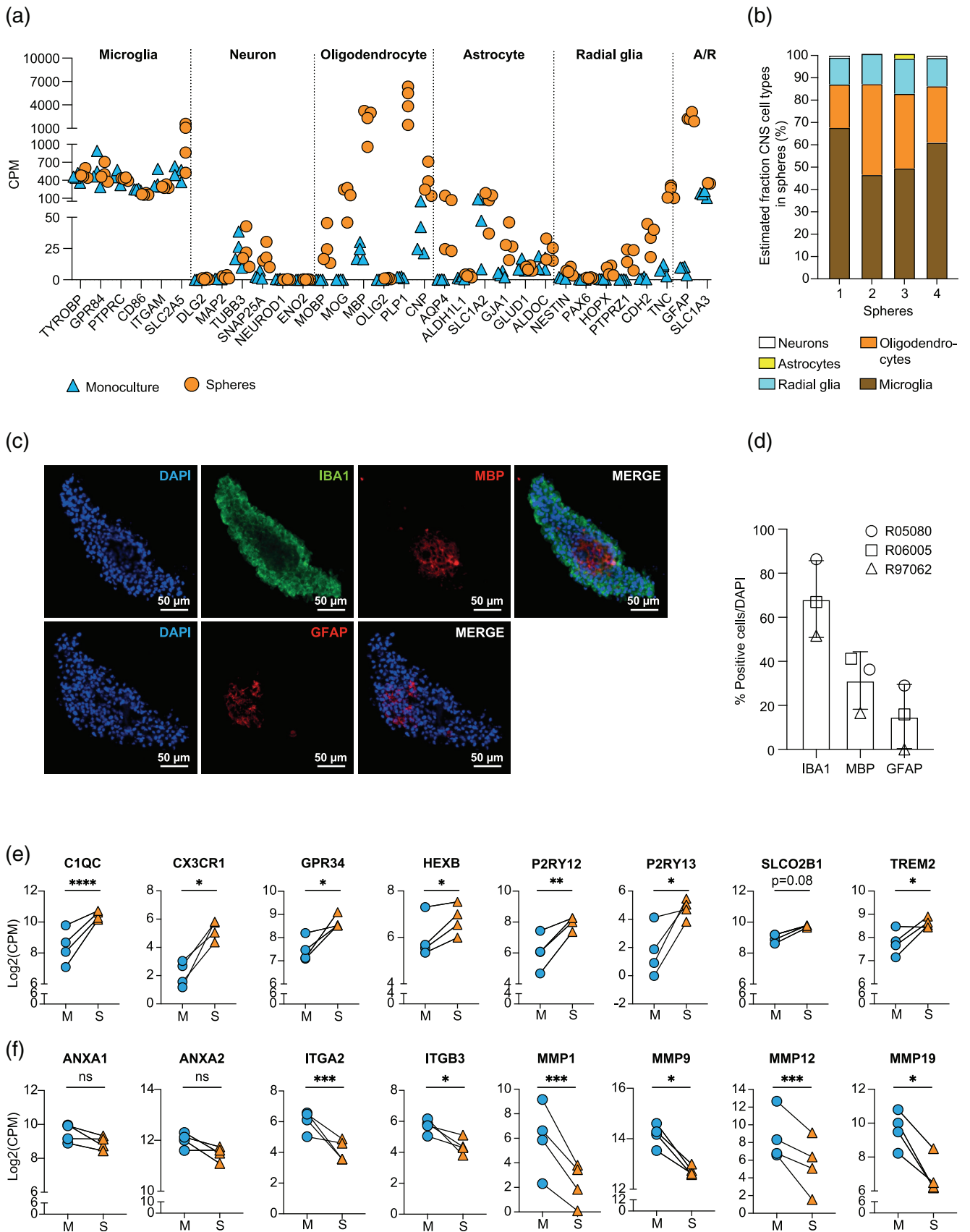


FIGURE 5 Legend on next page.

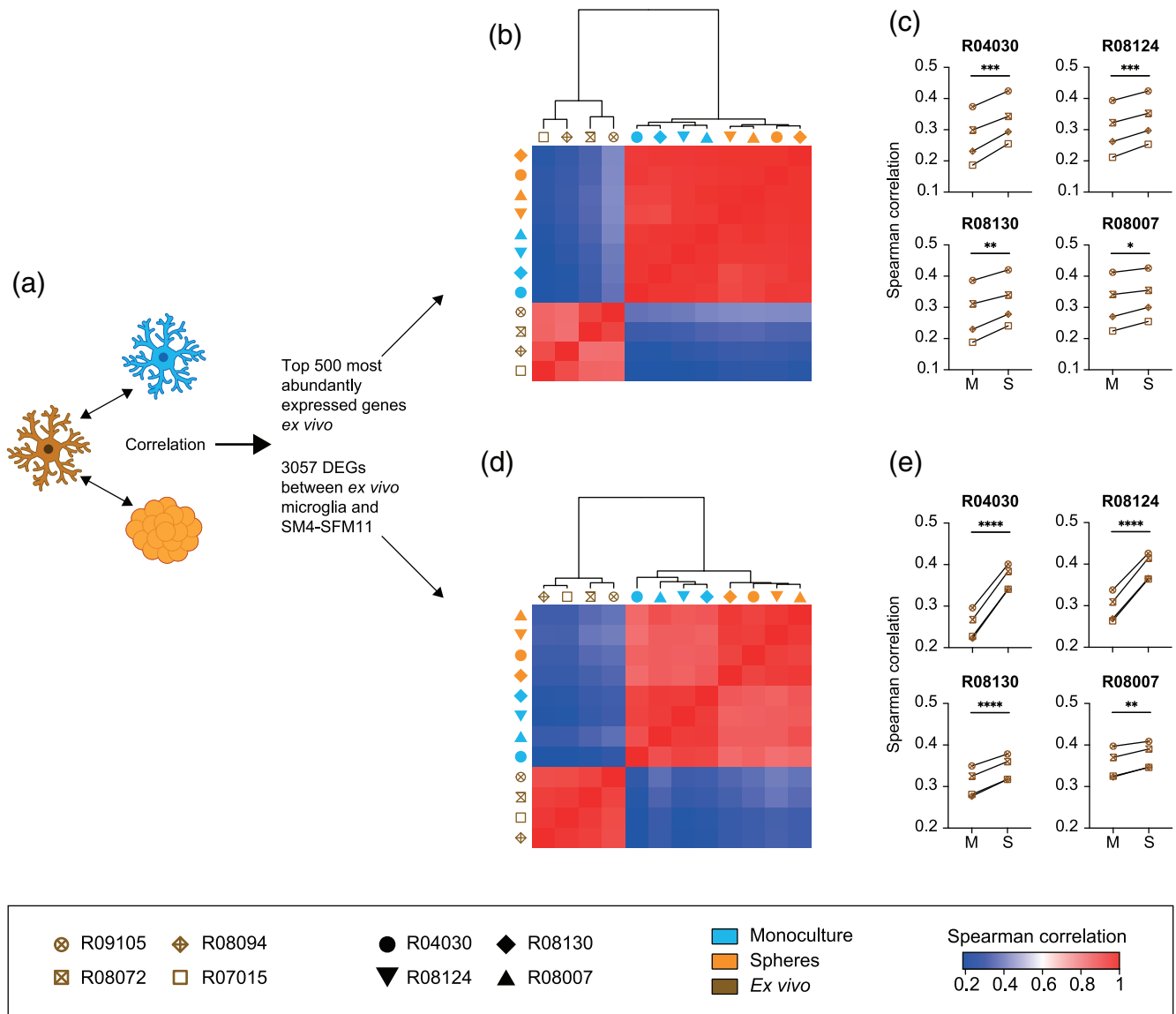


FIGURE 6 In-depth transcriptome analyses of microglia gene expression in spheres. (a) Overview of the transcriptome analytical approaches to gain further insight in the gene expression profile of microglia in spheres. (b) Spearman's correlation heatmap of the top 500 most abundantly expressed genes in ex vivo microglia. (c) Spearman's correlation values of Figure 6b between ex vivo microglia and monocultured microglia, and ex vivo microglia and spheres. $N = 4$, graph for each in vitro donor is displayed. $*p < .05$, $**p < .01$, $***p < .005$. M = monoculture, S = spheres. (d) Spearman's correlation heatmap of the 3057 genes that were differentially expressed between SM4-SFM11 microglia and ex vivo microglia. (e) Spearman's correlation values of Figure 6d between ex vivo microglia and monocultured microglia, and ex vivo microglia and spheres. $N = 4$, graph for each in vitro donor is displayed. $**p < .01$, $****p < .001$. M = monoculture, S = spheres

FIGURE 5 Characterization of primary cell-derived spheres. (a) Expression values (CPM) of microglia, neuron, oligodendrocyte, astrocyte and radial glia genes of SM4-SFM11 monocultured microglia and spheres ($n = 4$). A/R genes are genes both expressed by astrocytes and radial glia. (b) CIBERSORT (Newman et al., 2015) quantification analysis of the estimated numbers of neurons, astrocytes, radial glia, oligodendrocytes and microglia in spheres, $n = 4$. (c) One representative example of a sphere (R06005) immunostained with anti-IBA1 (as a microglia marker), with anti-MBP (as an oligodendrocyte marker), and with anti-GFAP (as a radial glia marker). Cell nuclei (blue) were visualized using 4',6-diamidino-2-phenylindole (DAPI). Scale bars represent 50 μm . (d) Estimated percentages of the different cell types in spheres plotted in a graph. Each symbol represents a donor. $N = 3$, error bars represent SD. (e) Log-transformed expression (CPM) values of microglia signature genes of microglia monocultures and spheres. EdgeR false discovery rates (FDR) are used to display statistical differences, $n = 4$, $*\text{FDR} < 0.05$, $**\text{FDR} < 0.01$, $****\text{FDR} < 0.001$. M = monoculture, S = spheres. (f) Log-transformed expression (CPM) values of extracellular matrix-related genes of microglia monocultures and spheres. EdgeR false discovery rates (FDR) are used to display statistical differences, $n = 4$, $*\text{FDR} < 0.05$, $****\text{FDR} < 0.01$. M = monoculture, S = spheres

CIBERSORT analysis, we visualized the expression of IBA1 (as a marker for microglia), MBP (as a marker for oligodendrocytes), and GFAP (as a marker for radial glia) (Figure 5c). Stainings were validated in the rhesus macaque source tissue (Figure S10a). Quantification confirmed that with $\pm 70\%$ microglia were the most abundant cell type in spheres followed by approximately 30% oligodendrocytes, and $\pm 10\%$ radial glia (Figure 5d). As GFAP is expressed both by astrocytes and by radial glia, we also analyzed the expression of Tenascin C (TNC), which is more selectively expressed by radial glia and by astrocytes precursor cells (Pollen et al., 2015; Wiese et al., 2012). Colocalization of GFAP and TNC in spheres (Figure S10b) are consistent with the idea that the GFAP-positive cells are radial glia.

Importantly, we observed that microglial signature genes *C1QC*, *CX3CR1*, *GPR34*, *HEXB*, *P2RY12*, *P2RY13*, and *TREM2* were significantly upregulated in spheres as compared to microglia monocultures (Figure 5e). It is noteworthy that bulk RNA-sequencing was used, meaning that the microglia in the spheres are likely to express even higher levels of these microglial-specific genes. Intriguingly, the expression levels of microglial genes *P2RY12*, *P2RY13*, and *CX3CR1* are thought to be regulated by neuron–microglia crosstalk, whereas we have no indications that neurons were present in our spheres. In addition, we analyzed the expression of neuronal progenitor genes. Although we found a significant upregulation of *SOX2* and *NES* in spheres (Figure S11), these two genes are also expressed by radial glia. As other neuronal progenitor genes, including *PAX6*, *OCT4*, *DCX*, *ASCL1*, and *MSI1* were not significantly upregulated in spheres, we found no evidence for the presence of neuronal progenitors in our spheres. Finally, we observed that the expression levels of *ITGA2*, *ITGB3*, *MMP1*, *MMP9*, *MMP12*, and *MMP19* were significantly downregulated in spheres as compared to microglia monocultures (Figure 5f).

3.7 | The gene expression profile of microglia in spheres better resembles that of ex vivo microglia

To gain a broader insight in the gene expression profile of microglia in spheres, we performed further transcriptome analyses (Figure 6a). As a first approach, we analyzed the expression of the top 500 most abundantly expressed genes in ex vivo microglia (listed in Table S5) and compared their expression levels to those in monocultured microglia and to those in spheres (Figure S12). Interestingly, Spearman's correlation analysis of these 500 genes show a higher correlation between spheres and ex vivo microglia than between monocultured microglia and ex vivo microglia (Figure 6b,c). As a second approach, we analyzed the expression of the 3057 genes that were differentially expressed (DEG; $FC \geq 4$, $FDR < 0.01$) between monocultured microglia (SM4-SFM11) and ex vivo microglia (Table 5). Again, Spearman's correlation analysis revealed an improvement of the expression of these 3057 genes in spheres for all four in vitro donors (Figure 6d,e). DEG analysis shows that of these 3057 genes, 159 genes were no longer differentially expressed ($FC \leq 4$, $FDR > 0.01$) between spheres and ex vivo microglia. Gene set enrichment analysis show that the majority of biological processes associated with these 159 genes are linked to neuronal

processes, such as neuron differentiation, neuron development and neurogenesis (Table S6). Together these data strongly suggest that microglia in spheres better mimic the gene expression profile of ex vivo microglia than monocultured microglia do.

4 | DISCUSSION

The increasing recognition of microglia as druggable cellular targets for a variety of neurodegenerative disorders, has spurred research into the determinants of microglial identity and into the development of in vitro methodology (Bohlen et al., 2017; Butovsky et al., 2014; Gosselin et al., 2017). In this study, we have exposed primary microglia from adult rhesus macaques to a variety of different cell culture regimes to shed light on the relative contribution of different cell culture methods and conditions in shaping microglial identity, and to further cell culture innovations.

The importance of the CSF-1 receptor for microglial proliferation, survival and homeostasis has been firmly established by different studies (Elmore et al., 2014; Erblich et al., 2011; Ginhoux et al., 2010; Oosterhof et al., 2018). The CSF-1 receptor has two reported ligands, M-CSF and IL-34, that lack similarity in terms of protein sequence and that are expressed in a largely non-overlapping manner in the brain (Greter et al., 2012; Wang et al., 2012; Wei et al., 2010). The idea that unique requirements exist for either M-CSF or IL-34 in the development, colonization and homeostasis of microglia, stems from observations made in depletion studies in rodents (Chitu et al., 2016; Easley-Neal et al., 2019; Wang et al., 2012) and zebrafish (Kuil et al., 2019; Wu et al., 2018). However, our results show that cell numbers and cellular morphologies (data not shown), as well as the transcriptomes, of primary microglia from adult primates exposed to either M-CSF or IL-34 were indistinguishable. These results are in line with those of a recent study in which the transcriptomes of primary microglia from adult humans exposed to either M-CSF or IL-34, were also reported to be almost identical (Walker et al., 2017). Taken together, these studies suggest similar roles for M-CSF and IL-34 in postnatal microglia homeostasis. It remains to be established though whether exposure of microglia to M-CSF or IL-34 can have an impact on the polarization towards a pro- or anti-inflammatory phenotype (Boulakirba et al., 2018), or on the susceptibility for infection with HIV (Paquin-Proulx et al., 2018), as has been described for human primary monocytes. If such effects were to be found in microglia as well, the heterogeneous expression of M-CSF and IL-34 in the brain (Chitu et al., 2016; Easley-Neal et al., 2019; Greter et al., 2012; Nakamichi et al., 2013) could lead to regional differences in microglia biology.

We also studied the effects of exposure to TGF- β , which is, both in vitro and in vivo, an important factor for microglia homeostasis and survival (Bohlen et al., 2017; Butovsky et al., 2014; Buttgeriet et al., 2016; Spittau et al., 2013; Zoller et al., 2018). Whereas in vitro exposure of microglia to TGF- β induces the expression of a transcriptome that better resembles that of mouse ex vivo microglia and, in addition, the expression of microglia signature genes (Butovsky et al., 2014), these effects were not reproduced in our system. This



was not attributable to a lack of engagement of TGF- β -induced signaling. Analysis of the expression of microglia signature genes demonstrates that only the expression of CX3CR1 was upregulated upon exposure to TGF- β , confirming the positive regulation of CX3CR1 by TGF- β (Chen et al., 2002; Wynne et al., 2010). The expression levels of *GPR34*, *P2RY13*, and *TMEM119* were unaffected, and expression levels of *P2RY12* and *OLFML3* were even downregulated after exposure to TGF- β . These data are in line with a study reporting on the modest effects of TGF- β exposure on primary cultured microglia from adolescent humans as compared to the effects on primary cultured microglia of 7–10 weeks old mice (Gosselin et al., 2017). Similar to our results, exposure to TGF- β did not result in a better match to the ex vivo transcriptome of human microglia. These important differences might be attributable to species-specific effects of TGF- β , as is also supported by the reported differences in TGF- β -mediated inhibition of IFN- γ -induced MHC class I expression in human and murine microglia (Smith et al., 2013). It is at present unclear where these differences originate, as the TGF- β superfamily is well conserved between rodents and humans (Hinck et al., 2016; Huminiacki et al., 2009).

We further observed that sex as a variable better explained variance in gene expression profiles than different culture conditions did. This is relevant given the sex-specific differences in the incidence, prevalence and pathogenesis of neurological diseases such as AD and MS (Barnes et al., 2005; Beam et al., 2018; Hanamsagar & Bilbo, 2016; Harbo et al., 2013; Nebel et al., 2018; Ploughman et al., 2017). Interestingly, sex-specific features in microglial function in health and disease have been identified in rodents (Acáz-Fonseca et al., 2015; Mapplebeck et al., 2018; Villa et al., 2018; Villapol et al., 2017). In line with earlier reported sex-specific DEGs in ex vivo human transcriptome data (Gosselin et al., 2017), analysis of the sex-specific DEGs in our in vitro transcriptome datasets shows that these were all localized to either the X- or the Y-chromosome (data not shown). In addition to sex, we observed considerable donor-donor variation in microglia transcriptomes. Although this is normal when working with material from an outbred population, and in line with reported variation in the transcriptomes of ex vivo human microglia (Alsema et al., 2020; Galatro, Holtman, et al., 2017; Gosselin et al., 2017; van der Poel et al., 2019), we had not expected to find such effects after prolonged in vitro culture periods under different regimes. This would suggest that donor-specific gene expression profiles in microglia remain relatively stable, which might hinder analyses of e.g. culture specific effects. It is at present not clear whether these sex and donor-specific differences can be related to differences in microglia biology or function.

Gene set enrichment analysis of our data uncovered that differences between the in vitro and ex vivo transcriptomes of microglia were for a considerable part attributable to gene transcripts associated with cell cycling, which could have been caused by in vitro exposure to serum. We therefore tested a recently described serum-free medium for rat microglia (Bohlen et al., 2017) on our primary rhesus macaque microglia in which it induced a complex, ramified, cell morphology accompanied by the reduced expression of genes associated

with proliferation. As the lack of proliferation negatively impacted the number of cells available for further in vitro experiments, we optimized a cell culture regime that combines a short-term, 4 day serum exposure with a serum-free washout period of at least 11 days. Although microglia are not exposed to serum in the healthy CNS, our results demonstrate that microglial responses to serum exposure are relative short-lived and appear to be for most part reversible. A minimum serum-free washout period of 11 days is sufficient to yield microglia with a highly complex, ramified morphology and with reduced expression levels of cell cycle-associated genes. In spite of these advances, the transcriptomes of microglia subjected to this new in vitro protocol still differed significantly from those of ex vivo microglia. Gene ontology analyses of the DEGs suggested that further improvements were among others to be found in exposure to the CNS microenvironment, in line with other studies (Bohlen et al., 2017; Svoboda et al., 2019).

We therefore facilitated the outgrowth of other brain-derived cells by plating our initial cell suspension in ultra-low attachment plates, which resulted in the formation of spheres. In such spheres, neuronal gene products could not be detected, whereas microglia, oligodendrocyte, astrocyte, and radial glia-specific gene products were easily detectable. Given the Percoll gradient-based isolation procedure we used, we think it is unlikely that astrocytes are present in our initial cell suspension. We favor the idea that the detection of astrocyte-specific gene products as *AQP4*, *GJA1*, and *GFAP* stems from neuronal or glial precursor cells, such as radial glia, which was also in line with the CIBERSORT analysis we performed and was further supported by immunofluorescence microscopical analysis.

In-depth transcriptome analyses demonstrate that the gene expression profile of microglia in spheres better resembles that of ex vivo microglia than those of monocultured microglia do. However, further studies, such as single cell RNA-sequencing, are required to confirm this. Most interestingly, the expression levels of many microglia signature genes were significantly enhanced in spheres, even of those genes thought to be regulated by neuron–microglia and astrocyte–microglia crosstalk. Whether this is the result of cell–cell contact, or of cell-derived soluble factors, warrants further investigation. At present, very little is known on the role of oligodendrocyte-derived and radial glia-derived soluble factors on microglia (Liu & Aguzzi, 2020), and this co-culture system can help to disentangle the intercellular communication that establishes and maintains microglial identity. As it has already been convincingly demonstrated that neuron–microglia and astrocyte–microglia communication positively affect microglia signature gene expression levels (Baxter et al., 2021; Matejuk & Ransohoff, 2020; Szepesi et al., 2018; Veremeyko et al., 2019), the addition of neurons and/or astrocytes to our spheres might even further increase the expression of microglial signature genes. Such a complex CNS culture model bears resemblance to the recently described cerebral organoids that were generated from induced pluripotent stem cells and that surprisingly also contained microglia (Ormel et al., 2018).

Taken together, our results provide new biological insights in cues that are important for adult primate microglial identity and for the development and optimization of novel in vitro methodology.

ACKNOWLEDGMENTS

We thank N. Brouwer and B. Eggen for ex vivo microglia isolation and RNA generation, H. Oostermeijer and S. Hofman for excellent technical flow-cytometrical support, E. Remarque for help with the statistical analyses, F. van Hassel for help with the graphical presentations of the research, T. Haaksmas and I. Kondova for help with the obductions and preparation of CNS material, and M. Hoonakker and I. Canals for critical feedback on the manuscript.

AUTHOR CONTRIBUTIONS

Conceptualization: Raissa Timmerman and Jeffrey J. Bajramovic; **Methodology:** Raissa Timmerman and Jeffrey J. Bajramovic; **Investigation:** Raissa Timmerman, Ella A. Zuiderwijk-Sick, Nynke Oosterhof, Anke E.J. 't Jong, Jennifer Veth, and Saskia M. Burm; **Formal analysis:** Raissa Timmerman; **Writing—Original Draft:** Raissa Timmerman and Jeffrey J. Bajramovic; **Writing—Review & Editing:** Raissa Timmerman, Nynke Oosterhof, Anke E.J. 't Jong, Saskia M. Burm, Tjakko J. van Ham, and Jeffrey J. Bajramovic; **Funding acquisition:** Jeffrey J. Bajramovic; **Supervision:** Jeffrey J. Bajramovic.

DATA AVAILABILITY STATEMENT

The data that support the findings of this study are available from the corresponding author upon reasonable request. The data that support the findings of the RNA sequencing in this study are openly available in GEO, reference number GSE171476.

ORCID

Raissa Timmerman  <https://orcid.org/0000-0002-1254-0931>

Tjakko J. van Ham  <https://orcid.org/0000-0002-2175-8713>

Jeffrey J. Bajramovic  <https://orcid.org/0000-0002-6504-3437>

REFERENCES

- Acaz-Fonseca, E., Duran, J. C., Carrero, P., Garcia-Segura, L. M., & Arevalo, M. A. (2015). Sex differences in glia reactivity after cortical brain injury. *Glia*, *63*(11), 1966–1981. <https://doi.org/10.1002/glia.22867>
- Aloisi, F. (2001). Immune function of microglia. *Glia*, *36*(2), 165–179. <https://doi.org/10.1002/glia.1106>
- Alsema, A. M., Jiang, Q., Kracht, L., Gerrits, E., Dubbelaar, M. L., Miedema, A., Brouwer, N., Hol, E. M., Middeldorp, J., van Dijk, R., Woodbury, M., Xi, S., Möller, T., Biber, K. P., Kooistra, S.M., Boddeke, E. W. G. M., & Eggen, B. J. L. (2020). Profiling microglia from Alzheimer's disease donors and non-demented elderly in acute human postmortem cortical tissue. *Frontiers in Molecular Neuroscience*, *13*, 134. <https://doi.org/10.3389/fnmol.2020.00134>
- Bajramovic, J. J. (2011). Regulation of innate immune responses in the central nervous system. *CNS & Neurological Disorders Drug Targets*, *10*(1), 4–24. <https://doi.org/10.2174/187152711794488610>
- Barnes, L. L., Wilson, R. S., Bienias, J. L., Schneider, J. A., Evans, D. A., & Bennett, D. A. (2005). Sex differences in the clinical manifestations of Alzheimer disease pathology. *Archives of General Psychiatry*, *62*(6), 685–691. <https://doi.org/10.1001/archpsyc.62.6.685>
- Baxter, P. S., Dando, O., Emelianova, K., He, X., McKay, S., Hardingham, G. E., & Qiu, J. (2021). Microglial identity and inflammatory responses are controlled by the combined effects of neurons and astrocytes. *Cell Reports*, *34*(12), 108882. <https://doi.org/10.1016/j.celrep.2021.108882>
- Beam, C. R., Kaneshiro, C., Jang, J. Y., Reynolds, C. A., Pedersen, N. L., & Gatz, M. (2018). Differences between women and men in incidence rates of dementia and Alzheimer's disease. *Journal of Alzheimer's Disease*, *64*(4), 1077–1083. <https://doi.org/10.3233/JAD-180141>
- Bennett, M. L., Bennett, F. C., Liddel, S. A., Ajami, B., Zamanian, J. L., Fernhoff, N. B., Mulinyawe, S. B., Bohlen, C. J., Adil, A., Tucker, A., Weissman, I. L., Chang, E. F., Li, G., Grant, G. A., Hayden Gephart, M. G., & Barres, B. A. (2016). New tools for studying microglia in the mouse and human CNS. *Proceedings of the National Academy of Sciences of the United States of America*, *113*(12), E1738–E1746. <https://doi.org/10.1073/pnas.1525528113>
- Bohlen, C. J., Bennett, F. C., Tucker, A. F., Collins, H. Y., Mulinyawe, S. B., & Barres, B. A. (2017). Diverse requirements for microglial survival, specification, and function revealed by defined-medium cultures. *Neuron*, *94*(4), 759–773 e758. <https://doi.org/10.1016/j.neuron.2017.04.043>
- Boulakirba, S., Pfeifer, A., Mhaidly, R., Obba, S., Goulard, M., Schmitt, T., Chaintreuil, P., Calleja, A., Furstoss, N., Orange, F., Lacas-Gervais, S., Boyer, L., Marchetti, S., Verhoeyen, E., Luciano, F., Robert, G., Auberger, P., & Jacquel, A. (2018). IL-34 and CSF-1 display an equivalent macrophage differentiation ability but a different polarization potential. *Scientific Reports*, *8*(1), 256. <https://doi.org/10.1038/s41598-017-18433-4>
- Burm, S. M., Zuiderwijk-Sick, E. A., Jong, A. E., van der Putten, C., Veth, J., Kondova, I., & Bajramovic, J. J. (2015). Inflammasome-induced IL-1beta secretion in microglia is characterized by delayed kinetics and is only partially dependent on inflammatory caspases. *The Journal of Neuroscience*, *35*(2), 678–687. <https://doi.org/10.1523/JNEUROSCI.2510-14.2015>
- Burm, S. M., Zuiderwijk-Sick, E. A., Weert, P. M., & Bajramovic, J. J. (2016). ATP-induced IL-1beta secretion is selectively impaired in microglia as compared to hematopoietic macrophages. *Glia*, *64*(12), 2231–2246. <https://doi.org/10.1002/glia.23059>
- Butovsky, O., Jedrychowski, M. P., Moore, C. S., Cialic, R., Lanser, A. J., Gabriely, G., Koeglsperger, T., Dake, B., Wu, P. M., Doykan, C. E., Fanek, Z., Liu, L., Chen, Z., Rothstein, J. D., Ransohoff, R. M., Gygi, S. P., Antel, J. P., & Weiner, H. L. (2014). Identification of a unique TGF-beta-dependent molecular and functional signature in microglia. *Nature Neuroscience*, *17*(1), 131–143. <https://doi.org/10.1038/nn.3599>
- Buttgereit, A., Lelios, I., Yu, X., Vrohlig, M., Krakoski, N. R., Gautier, E. L., Nishinakamura, R., Burkhard Becher, B., & Greter, M. (2016). Sall1 is a transcriptional regulator defining microglia identity and function. *Nature Immunology*, *17*(12), 1397–1406. <https://doi.org/10.1038/ni.3585>
- Chen, S., Luo, D., Streit, W. J., & Harrison, J. K. (2002). TGF-beta1 upregulates CX3CR1 expression and inhibits fractalkine-stimulated signaling in rat microglia. *Journal of Neuroimmunology*, *133*(1–2), 46–55. [https://doi.org/10.1016/s0165-5728\(02\)00354-5](https://doi.org/10.1016/s0165-5728(02)00354-5)
- Chitu, V., Gokhan, S., Nandi, S., Mehler, M. F., & Stanley, E. R. (2016). Emerging roles for CSF-1 receptor and its ligands in the nervous system. *Trends in Neurosciences*, *39*(6), 378–393. <https://doi.org/10.1016/j.tins.2016.03.005>
- Crotti, A., & Ransohoff, R. M. (2016). Microglial physiology and pathophysiology: Insights from genome-wide transcriptional profiling. *Immunity*, *44*(3), 505–515. <https://doi.org/10.1016/j.immuni.2016.02.013>
- Cserep, C., Posfai, B., Lenart, N., Fekete, R., Laszlo, Z. I., Lele, Z., Orsolits, B., Molnár, G., Heindl, S., Schwarcz, A. D., Ujvári, K., Kőrnyei, Z., Tóth, K., Szabadits, E., Sperlágh, B., Baranyi, M., Csiba, L., Hortobágyi, T., Maglóczy, ... Denes, A. (2020). Microglia monitor and protect neuronal function through specialized somatic purinergic junctions. *Science*, *367*(6477), 528–537. <https://doi.org/10.1126/science.aax6752>
- Durinck, S., Moreau, Y., Kasprzyk, A., Davis, S., De Moor, B., Brazma, A., & Huber, W. (2005). BioMart and bioconductor: A powerful link between biological databases and microarray data analysis. *Bioinformatics*, *21*(16), 3439–3440. <https://doi.org/10.1093/bioinformatics/bti525>



- Durinck, S., Spellman, P. T., Birney, E., & Huber, W. (2009). Mapping identifiers for the integration of genomic datasets with the R/bioconductor package biomaRt. *Nature Protocols*, 4(8), 1184–1191. <https://doi.org/10.1038/nprot.2009.97>
- Easley-Neal, C., Foreman, O., Sharma, N., Zarrin, A. A., & Weimer, R. M. (2019). CSF1R ligands IL-34 and CSF1 are differentially required for microglia development and maintenance in White and gray matter brain regions. *Frontiers in Immunology*, 10, 2199. <https://doi.org/10.3389/fimmu.2019.02199>
- Elmore, M. R., Najafi, A. R., Koike, M. A., Dagher, N. N., Spangenberg, E. E., Rice, R. A., Kitazawa, M., Matusow, B., Nguyen, H., West, B. L., & Green, K. N. (2014). Colony-stimulating factor 1 receptor signaling is necessary for microglia viability, unmasking a microglia progenitor cell in the adult brain. *Neuron*, 82(2), 380–397. <https://doi.org/10.1016/j.neuron.2014.02.040>
- Erblich, B., Zhu, L., Etgen, A. M., Dobrenis, K., & Pollard, J. W. (2011). Absence of colony stimulation factor-1 receptor results in loss of microglia, disrupted brain development and olfactory deficits. *PLoS One*, 6(10), e26317. <https://doi.org/10.1371/journal.pone.0026317>
- Eun, S. Y., Hong, Y. H., Kim, E. H., Jeon, H., Suh, Y. H., Lee, J. E., Jo, C., Jo, S. A., & Kim, J. (2004). Glutamate receptor-mediated regulation of c-fos expression in cultured microglia. *Biochemical and Biophysical Research Communications*, 325(1), 320–327. <https://doi.org/10.1016/j.bbrc.2004.10.035>
- Ferreira, T. A., Blackman, A. V., Oyrer, J., Jayabal, S., Chung, A. J., Watt, A. J., Sjöström, P. J., & van Meyel, D. J. (2014). Neuronal morphology directly from bitmap images. *Nature Methods*, 11(10), 982–984. <https://doi.org/10.1038/nmeth.3125>
- Galatro, T. F., Holtman, I. R., Lerario, A. M., Vainchtein, I. D., Brouwer, N., Sola, P. R., Veras, M. M., Pereira, T. F., Leite, R. E. P., Möller, T., Wes, P. D., Sogayar, M. C., Laman, J. D., den Dunnen, W., Pasqualucci, C. A., Oba-Shinjo, S. M., Boddeke, E. W. G. M., Marie, S. K. N., Eggen, B. J. L., & Eggen, B. J. L. (2017). Transcriptomic analysis of purified human cortical microglia reveals age-associated changes. *Nature Neuroscience*, 20(8), 1162–1171. <https://doi.org/10.1038/nn.4597>
- Galatro, T. F., Vainchtein, I. D., Brouwer, N., Boddeke, E., & Eggen, B. J. L. (2017). Isolation of microglia and immune infiltrates from mouse and primate central nervous system. *Methods in Molecular Biology*, 1559, 333–342. https://doi.org/10.1007/978-1-4939-6786-5_23
- Ginhoux, F., Greter, M., Leboeuf, M., Nandi, S., See, P., Gokhan, S., Mehler, M. F., Conway, S. J., Ng, L. G., Stanley, E. R., Samokhvalov, I. M., Merad, M., & Merad, M. (2010). Fate mapping analysis reveals that adult microglia derive from primitive macrophages. *Science*, 330(6005), 841–845. <https://doi.org/10.1126/science.1194637>
- Gosselin, D., Skola, D., Coufal, N. G., Holtman, I. R., Schlachetzki, J. C. M., Sajti, E., Jaeger, B. N., O'Connor, C., Fitzpatrick, C., Pasillas, M. P., Pena, M., Adair, A., Gonda, D. D., Levy, M. L., Ransohoff, R. M., Gage, F. H., & Glass, C. K. (2017). An environment-dependent transcriptional network specifies human microglia identity. *Science*, 356(6344), 2017–2023. <https://doi.org/10.1126/science.aal3222>
- Greter, M., Lelios, I., Pelczar, P., Hoeffel, G., Price, J., Leboeuf, M., Kündig, T. M., Frei, K., Ginhoux, F., Merad, M., & Becher, B. (2012). Stromal-derived interleukin-34 controls the development and maintenance of langerhans cells and the maintenance of microglia. *Immunity*, 37(6), 1050–1060. <https://doi.org/10.1016/j.immuni.2012.11.001>
- Hall, E. D., Oostveen, J. A., & Gurney, M. E. (1998). Relationship of microglial and astrocytic activation to disease onset and progression in a transgenic model of familial ALS. *Glia*, 23(3), 249–256. [https://doi.org/10.1002/\(SICI\)1098-1136\(199807\)23:3<249::AID-GLIA7>3.0.CO;2-%23](https://doi.org/10.1002/(SICI)1098-1136(199807)23:3<249::AID-GLIA7>3.0.CO;2-%23)
- Hanamsagar, R., & Bilbo, S. D. (2016). Sex differences in neurodevelopmental and neurodegenerative disorders: Focus on microglial function and neuroinflammation during development. *The Journal of Steroid Biochemistry and Molecular Biology*, 160, 127–133. <https://doi.org/10.1016/j.jsbmb.2015.09.039>
- Harbo, H. F., Gold, R., & Tintore, M. (2013). Sex and gender issues in multiple sclerosis. *Therapeutic Advances in Neurological Disorders*, 6(4), 237–248. <https://doi.org/10.1177/1756285613488434>
- Haukedal, H., & Freude, K. (2019). Implications of microglia in amyotrophic lateral sclerosis and Frontotemporal dementia. *Journal of Molecular Biology*, 431(9), 1818–1829. <https://doi.org/10.1016/j.jmb.2019.02.004>
- Heneka, M. T., Kummer, M. P., & Latz, E. (2014). Innate immune activation in neurodegenerative disease. *Nature Reviews. Immunology*, 14(7), 463–477. <https://doi.org/10.1038/nri3705>
- Hinck, A. P., Mueller, T. D., & Springer, T. A. (2016). Structural biology and evolution of the TGF-beta family. *Cold Spring Harbor Perspectives in Biology*, 8(12), 1–51. <https://doi.org/10.1101/cshperspect.a022103>
- Huminiecki, L., Goldovsky, L., Freilich, S., Moustakas, A., Ouzounis, C., & Heldin, C. H. (2009). Emergence, development and diversification of the TGF-beta signalling pathway within the animal kingdom. *BMC Evolutionary Biology*, 9, 28. <https://doi.org/10.1186/1471-2148-9-28>
- Karch, C. M., & Goate, A. M. (2015). Alzheimer's disease risk genes and mechanisms of disease pathogenesis. *Biological Psychiatry*, 77(1), 43–51. <https://doi.org/10.1016/j.biopsych.2014.05.006>
- Kim, Y. S., & Joh, T. H. (2006). Microglia, major player in the brain inflammation: Their roles in the pathogenesis of Parkinson's disease. *Experimental & Molecular Medicine*, 38(4), 333–347. <https://doi.org/10.1038/emm.2006.40>
- Kober, D. L., & Brett, T. J. (2017). TREM2-ligand interactions in Health and disease. *Journal of Molecular Biology*, 429(11), 1607–1629. <https://doi.org/10.1016/j.jmb.2017.04.004>
- Kuil, L. E., Oosterhof, N., Geurts, S. N., van der Linde, H. C., Meijering, E., & van Ham, T. J. (2019). Reverse genetic screen reveals that IL34 facilitates yolk sac macrophage distribution and seeding of the brain. *Disease Models & Mechanisms*, 12(3), 1–29. <https://doi.org/10.1242/dmm.037762>
- Li, Q., & Barres, B. A. (2018). Microglia and macrophages in brain homeostasis and disease. *Nature Reviews. Immunology*, 18(4), 225–242. <https://doi.org/10.1038/nri.2017.125>
- Liberzon, A., Subramanian, A., Pinchback, R., Thorvaldsdottir, H., Tamayo, P., & Mesirov, J. P. (2011). Molecular signatures database (MSigDB) 3.0. *Bioinformatics*, 27(12), 1739–1740. <https://doi.org/10.1093/bioinformatics/btr260>
- Liu, Y., & Aguzzi, A. (2020). NG2 glia are required for maintaining microglia homeostatic state. *Glia*, 68(2), 345–355. <https://doi.org/10.1002/glia.23721>
- Longair, M. H., Baker, D. A., & Armstrong, J. D. (2011). Simple Neurite tracer: Open source software for reconstruction, visualization and analysis of neuronal processes. *Bioinformatics*, 27(17), 2453–2454. <https://doi.org/10.1093/bioinformatics/btr390>
- Mapplebeck, J. C. S., Dalgarno, R., Tu, Y., Moriarty, O., Beggs, S., Kwok, C. H. T., Halievski, K., Assi, S., Mogil, J. S., Trang, T., & Salter, M. W. (2018). Microglial P2X4R-evoked pain hypersensitivity is sexually dimorphic in rats. *Pain*, 159(9), 1752–1763. <https://doi.org/10.1097/j.pain.0000000000001265>
- Matejuk, A., & Ransohoff, R. M. (2020). Crosstalk between astrocytes and microglia: An overview. *Frontiers in Immunology*, 11, 1416. <https://doi.org/10.3389/fimmu.2020.01416>
- McGeer, P. L., Itagaki, S., Boyes, B. E., & McGeer, E. G. (1988). Reactive microglia are positive for HLA-DR in the substantia nigra of Parkinson's and Alzheimer's disease brains. *Neurology*, 38(8), 1285–1291. <https://doi.org/10.1212/wnl.38.8.1285>
- Mizee, M. R., Miedema, S. S., van der Poel, M., Adelia, S., van Strien, K. G., Melief, J., Smolders, J., Hendrickx, D. A., Heutinck, K. M., Hamann, J., & Huitinga, I. (2017). Isolation of primary microglia from the human post-mortem brain: Effects of ante- and post-mortem variables. *Acta Neuropathologica Communications*, 5(1), 16. <https://doi.org/10.1186/s40478-017-0418-8>

- Morrison, H., Young, K., Qureshi, M., Rowe, R. K., & Lifshitz, J. (2017). Quantitative microglia analyses reveal diverse morphologic responses in the rat cortex after diffuse brain injury. *Scientific Reports*, 7(1), 13211. <https://doi.org/10.1038/s41598-017-13581-z>
- Nakamichi, Y., Udagawa, N., & Takahashi, N. (2013). IL-34 and CSF-1: Similarities and differences. *Journal of Bone and Mineral Metabolism*, 31(5), 486–495. <https://doi.org/10.1007/s00774-013-0476-3>
- Nebel, R. A., Aggarwal, N. T., Barnes, L. L., Gallagher, A., Goldstein, J. M., Kantarci, K., Mallampalli, M. P., Mormino, E. C., Scott, L., Yu, W. H., Maki, P. M., & Mielke, M. M. (2018). Understanding the impact of sex and gender in Alzheimer's disease: A call to action. *Alzheimers Dement*, 14(9), 1171–1183. <https://doi.org/10.1016/j.jalz.2018.04.008>
- Neidert, N., von Ehr, A., Zoller, T., & Spittau, B. (2018). Microglia-specific expression of Olfml3 is directly regulated by transforming growth factor beta1-induced Smad2 signaling. *Frontiers in Immunology*, 9, 1728. <https://doi.org/10.3389/fimmu.2018.01728>
- Newman, A. M., Liu, C. L., Green, M. R., Gentles, A. J., Feng, W., Xu, Y., Hoang, C. D., Diehn, M., & Alizadeh, A. A. (2015). Robust enumeration of cell subsets from tissue expression profiles. *Nature Methods*, 12(5), 453–457. <https://doi.org/10.1038/nmeth.3337>
- Olah, M., Patrick, E., Villani, A. C., Xu, J., White, C. C., Ryan, K. J., Piehowski, P., Kapasi, A., Nejad, P., Cimpean, M., Connor, S., Yung, C. J., Frangieh, M., McHenry, A., Elyaman, W., Petyuk, V., Schneider, J. A., Bennett, D. A., De Jager, P. L., & Bradshaw, E. M. (2018). A transcriptomic atlas of aged human microglia. *Nature Communications*, 9(1), 539. <https://doi.org/10.1038/s41467-018-02926-5>
- Oosterhof, N., Kuil, L. E., van der Linde, H. C., Burm, S. M., Berdowski, W., van Ijcken, W. F. J., van Swieten, J. C., Hol, E. M., Verheijen, M. H. G., & van Ham, T. J. (2018). Colony-stimulating factor 1 receptor (CSF1R) regulates microglia density and distribution, but not microglia differentiation in vivo. *Cell Reports*, 24(5), 1203–1217 e1206. <https://doi.org/10.1016/j.celrep.2018.06.113>
- Ormel, P. R., Vieira de Sa, R., van Bodegraven, E. J., Karst, H., Harschnitz, O., Sneebouer, M. A. M., Johansen, L. E., van Dijk, R. E., Scheefhals, N., van Berlekom, A. B., Martínez, E. R., Kling, S., MacGillavry, H. D., van den Berg, L. H., Kahn, R. S., Hol, E. M., de Witte, L. D., & Pasterkamp, R. J. (2018). Microglia innately develop within cerebral organoids. *Nature Communications*, 9(1), 4167. <https://doi.org/10.1038/s41467-018-06684-2>
- Paolicelli, R. C., Bolasco, G., Pagani, F., Maggi, L., Scianni, M., Panzanelli, P., Giustetto, M., Ferreira, T. A., Guiducci, E., Dumas, L., Ragozzino, D., & Gross, C. T. (2011). Synaptic pruning by microglia is necessary for normal brain development. *Science*, 333(6048), 1456–1458. <https://doi.org/10.1126/science.1202529>
- Paquin-Proulx, D., Greenspun, B. C., Kitchen, S. M., Saraiva Raposo, R. A., Nixon, D. F., & Grayfer, L. (2018). Human interleukin-34-derived macrophages have increased resistance to HIV-1 infection. *Cytokine*, 111, 272–277. <https://doi.org/10.1016/j.cyto.2018.09.006>
- Patir, A., Shih, B., McColl, B. W., & Freeman, T. C. (2019). A core transcriptional signature of human microglia: Derivation and utility in describing region-dependent alterations associated with Alzheimer's disease. *Glia*, 67(7), 1240–1253. <https://doi.org/10.1002/glia.23572>
- Perry, V. H., Nicoll, J. A., & Holmes, C. (2010). Microglia in neurodegenerative disease. *Nature Reviews. Neurology*, 6(4), 193–201. <https://doi.org/10.1038/nrneurol.2010.17>
- Ploughman, M., Collins, K., Wallack, E. M., Monks, M., Mayo, N., Health, L., & Aging with, M. S. C. C. (2017). Women's and Men's differing experiences of Health, lifestyle, and aging with multiple sclerosis. *The International Journal of MS Care*, 19(4), 165–171. <https://doi.org/10.7224/1537-2073.2016-014>
- Pollen, A. A., Nowakowski, T. J., Chen, J., Retallack, H., Sandoval-Espinosa, C., Nicholas, C. R., Shuga, J., Liu, S. J., Oldham, M. C., Diaz, A., Lim, D. A., Leyrat, A. A., West, J. A., & Kriegstein, A. R. (2015). Molecular identity of human outer radial glia during cortical development. *Cell*, 163(1), 55–67. <https://doi.org/10.1016/j.cell.2015.09.004>
- Robinson, M. D., McCarthy, D. J., & Smyth, G. K. (2010). edgeR: A bioconductor package for differential expression analysis of digital gene expression data. *Bioinformatics*, 26(1), 139–140. <https://doi.org/10.1093/bioinformatics/btp616>
- Sheridan, G. K., & Murphy, K. J. (2013). Neuron-glia crosstalk in health and disease: Fractalkine and CX3CR1 take Centre stage. *Open Biology*, 3(12), 130181. <https://doi.org/10.1098/rsob.130181>
- Smith, A. M., Graham, E. S., Feng, S. X., Oldfield, R. L., Bergin, P. M., Mee, E. W., Faull, R. L. M., Curtis, M. A., & Draganow, M. (2013). Adult human glia, pericytes and meningeal fibroblasts respond similarly to IFN γ but not to TGF β 1 or M-CSF. *PLoS One*, 8(12), e80463. <https://doi.org/10.1371/journal.pone.0080463>
- Spittau, B., Wullkopf, L., Zhou, X., Rilka, J., Pfeifer, D., & Kriegstein, K. (2013). Endogenous transforming growth factor-beta promotes quiescence of primary microglia in vitro. *Glia*, 61(2), 287–300. <https://doi.org/10.1002/glia.22435>
- Subramanian, A., Tamayo, P., Mootha, V. K., Mukherjee, S., Ebert, B. L., Gillette, M. A., Paulovich, A., Pomeroy, S. L., Golub, T. R., Lander, E. S., & Mesirov, J. P. (2005). Gene set enrichment analysis: A knowledge-based approach for interpreting genome-wide expression profiles. *Proceedings of the National Academy of Sciences of the United States of America*, 102(43), 15545–15550. <https://doi.org/10.1073/pnas.0506580102>
- Svoboda, D. S., Barrasa, M. I., Shu, J., Rietjens, R., Zhang, S., Mitalipova, M., Berube, P., Fu, D., Shultz, L. D., Bell, G. W., & Jaenisch, R. (2019). Human iPSC-derived microglia assume a primary microglia-like state after transplantation into the neonatal mouse brain. *Proceedings of the National Academy of Sciences of the United States of America*, 116(50), 25293–25303. <https://doi.org/10.1073/pnas.1913541116>
- Szepesi, Z., Manouchehrian, O., Bachiller, S., & Deierborg, T. (2018). Bidirectional microglia-neuron communication in Health and disease. *Frontiers in Cellular Neuroscience*, 12, 323. <https://doi.org/10.3389/fncel.2018.00323>
- Timmerman, R., Burm, S. M., & Bajramovic, J. J. (2018). An overview of in vitro methods to study microglia. *Frontiers in Cellular Neuroscience*, 12, 242. <https://doi.org/10.3389/fncel.2018.00242>
- Timmerman, R., Burm, S. M., & Bajramovic, J. J. (2021). Tissue-specific features of microglial innate immune responses. *Neurochemistry International*, 142, 104924. <https://doi.org/10.1016/j.neuint.2020.104924>
- van der Poel, M., Ulas, T., Mizze, M. R., Hsiao, C. C., Miedema, S. S. M., Adelia, A., Schuurman, K. G., Helder, B., Tas, S. W., Schultze, J. L., Hamann, J., & Huitinga, I. (2019). Transcriptional profiling of human microglia reveals grey-white matter heterogeneity and multiple sclerosis-associated changes. *Nature Communications*, 10(1), 1139. <https://doi.org/10.1038/s41467-019-08976-7>
- Van Der Putten, C., Kuipers, H. F., Zuiderwijk-Sick, E. A., Van Straalen, L., Kondova, I., Van Den Elsen, P. J., & Bajramovic, J. J. (2012). Statins amplify TLR-induced responses in microglia via inhibition of cholesterol biosynthesis. *Glia*, 60(1), 43–52. <https://doi.org/10.1002/glia.21245>
- van der Putten, C., Zuiderwijk-Sick, E. A., van Straalen, L., de Geus, E. D., Boven, L. A., Kondova, I., IJzerman, A. P., & Bajramovic, J. J. (2009). Differential expression of adenosine A3 receptors controls adenosine A2A receptor-mediated inhibition of TLR responses in microglia. *Journal of Immunology*, 182(12), 7603–7612. <https://doi.org/10.4049/jimmunol.0803383>
- Veremeyko, T., Yung, A. W. Y., Dukhinova, M., Strelakova, T., & Ponomarev, E. D. (2019). The role of neuronal factors in the epigenetic reprogramming of microglia in the Normal and diseased central nervous system. *Frontiers in Cellular Neuroscience*, 13, 453. <https://doi.org/10.3389/fncel.2019.00453>
- Villa, A., Gelosa, P., Castiglioni, L., Cimino, M., Rizzi, N., Pepe, G., Lolli, F., Marcello, E., Sironi, L., Vegeto, E., & Maggi, A. (2018). Sex-specific

- features of microglia from adult mice. *Cell Reports*, 23(12), 3501–3511. <https://doi.org/10.1016/j.celrep.2018.05.048>
- Villapol, S., Loane, D. J., & Burns, M. P. (2017). Sexual dimorphism in the inflammatory response to traumatic brain injury. *Glia*, 65(9), 1423–1438. <https://doi.org/10.1002/glia.23171>
- Walker, D. G., Tang, T. M., & Lue, L. F. (2017). Studies on Colony stimulating factor Receptor-1 and ligands Colony stimulating Factor-1 and Interleukin-34 in Alzheimer's disease brains and human microglia. *Frontiers in Aging Neuroscience*, 9, 244. <https://doi.org/10.3389/fnagi.2017.00244>
- Wang, Y., Szretter, K. J., Vermi, W., Gilfillan, S., Rossini, C., Cella, M., Barrow, A. D., Diamond, M. S., & Colonna, M. (2012). IL-34 is a tissue-restricted ligand of CSF1R required for the development of Langerhans cells and microglia. *Nature Immunology*, 13(8), 753–760. <https://doi.org/10.1038/ni.2360>
- Wei, S., Nandi, S., Chitu, V., Yeung, Y. G., Yu, W., Huang, M., Williams, L. T., Lin, H., & Stanley, E. R. (2010). Functional overlap but differential expression of CSF-1 and IL-34 in their CSF-1 receptor-mediated regulation of myeloid cells. *Journal of Leukocyte Biology*, 88(3), 495–505. <https://doi.org/10.1189/jlb.1209822>
- Wiese, S., Karus, M., & Faissner, A. (2012). Astrocytes as a source for extracellular matrix molecules and cytokines. *Frontiers in Pharmacology*, 3, 120. <https://doi.org/10.3389/fphar.2012.00120>
- Wu, S., Xue, R., Hassan, S., Nguyen, T. M. L., Wang, T., Pan, H., Xu, J., Liu, Q., Zhang, W., & Wen, Z. (2018). Il34-Csf1r pathway regulates the migration and colonization of microglial precursors. *Developmental Cell*, 46(5), 552–563 e554. <https://doi.org/10.1016/j.devcel.2018.08.005>
- Wynne, A. M., Henry, C. J., Huang, Y., Cleland, A., & Godbout, J. P. (2010). Protracted downregulation of CX3CR1 on microglia of aged mice after lipopolysaccharide challenge. *Brain, Behavior, and Immunity*, 24(7), 1190–1201. <https://doi.org/10.1016/j.bbi.2010.05.011>
- Young, K., & Morrison, H. (2018). Quantifying microglia morphology from photomicrographs of immunohistochemistry prepared tissue using ImageJ. *The Journal of Visualized Experiments*, 136, 1–9. <https://doi.org/10.3791/57648>
- Zhang, Y., Chen, K., Sloan, S. A., Bennett, M. L., Scholze, A. R., O'Keefe, S., Phatnani, H. P., Guarnieri, P., Caneda, C., Ruderisch, N., Deng, S., Liddelow, S. A., Zhang, C., Daneman, R., Maniatis, T., Barres, B. A., & Wu, J. Q. (2014). An RNA-sequencing transcriptome and splicing database of glia, neurons, and vascular cells of the cerebral cortex. *The Journal of Neuroscience*, 34(36), 11929–11947. <https://doi.org/10.1523/JNEUROSCI.1860-14.2014>
- Zhang, Y., Sloan, S. A., Clarke, L. E., Caneda, C., Plaza, C. A., Blumenthal, P. D., Vogel, H., Steinberg, G. K., Edwards, M. S. B., Li, G., Duncan, J. A., Cheshier, S. H., Shuer, L. M., Chang, E. F., Grant, G. A., Hayden Gephart, M. G., & Barres, B. A. (2016). Purification and characterization of progenitor and mature human astrocytes reveals transcriptional and functional differences with mouse. *Neuron*, 89(1), 37–53. <https://doi.org/10.1016/j.neuron.2015.11.013>
- Zoller, T., Schneider, A., Kleimeyer, C., Masuda, T., Potru, P. S., Pfeifer, D., Blank, T., Prinz, M., & Spittau, B. (2018). Silencing of TGFbeta signaling in microglia results in impaired homeostasis. *Nature Communications*, 9(1), 4011. <https://doi.org/10.1038/s41467-018-06224-y>
- Zuiderwijk-Sick, E. A., van der Putten, C., Bsibsi, M., Deuzing, I. P., de Boer, W., Persoon-Deen, C., Kondova, I., Boven, L. A., van Noort, J. M., A 't Hart, B., Amor, S., & Bajramovic, J. J. (2007). Differentiation of primary adult microglia alters their response to TLR8-mediated activation but not their capacity as APC. *Glia*, 55(15), 1589–1600. <https://doi.org/10.1002/glia.20572>

SUPPORTING INFORMATION

Additional supporting information may be found in the online version of the article at the publisher's website.

How to cite this article: Timmerman, R., Zuiderwijk-Sick, E. A., Oosterhof, N., 't Jong, A. E. J., Veth, J., Burm, S. M., van Ham, T. J., & Bajramovic, J. J. (2022). Transcriptome analysis reveals the contribution of oligodendrocyte and radial glia-derived cues for maintenance of microglia identity. *Glia*, 1–20. <https://doi.org/10.1002/glia.24136>